UNIVERSITY OF TURIN

Ph.D. School in Life and Health Sciences

Molecular Medicine

XXXIII Cycle

Genetic and pharmacological modulation of DNA mismatch repair promotes immune surveillance in murine colorectal cancer

Tutor:

Prof. Alberto Bardelli

Candidato:

Vito Amodio

Coordinator:

Prof. Francesco Novelli

TABLE OF CONTENTS

1. ABSTRACT 5

2. INTRODUCTION 6

2.1 Microsatellite stable and microsatellite instable colorectal cancer 6

2.2 Mutational characteristics of mismatch-repair-deficient cancer cell 7

2.3 CRC MMR status and immune surveillance 8

2.3.1 Neoantigen-dependent activation of immune surveillance in MMR-deficient colorectal cancers 11

2.4 Treatment with checkpoint inhibitors in MSS and MSI mCRC patients 14

2.5 Cytosolic DNA release contributes to the immunogenic properties of MMRd tumors 15

2.6 Intra-tumoral genetic diversity of the MMR Status 18

2.7 MMR heterogeneity and immune surveillance 21

2.8 Exploiting MMR heterogeneity for CRC immunotherapy 22

3. AIM OF THE STUDY 26

4. MATERIAL AND METHODS 27

4.1 Mouse cell lines 27

4.2 Gene editing 27

4.3 Animal studies 28

4.4 Mice treatment 28

4.5 Western Blot analyses 29

4.6 Genomic DNA extraction 29

4.7 Droplet digital PCR detection 30

4.8 In vitro enrichment assay 31

4.9 Immunophenotyping 31

4.10 Statistics 31

5. RESULTS 32

5.1 The MMRd component affects the growth of MMRd/MMRp heterogenous tumors 34

5.2 Tumor growth delay is immune driven in MMR heterogeneous CT26 36

5.3 Modulation of the local tumor immune microenvironment by MMR deficient cells is key for immune surveillance. 38

5.4 Profiling the immunological milieu of MMR heterogeneous tumor 40

5.5 Immune escape of MMR heterogeneous tumors is driven by the MMR proficient fraction 41

5.6 6-thioguanine and Temozolomide treatments of MMR heterogeneous tumors enriche for the MMRd deficient component and improve immune surveillance 44

5.7 In vivo 6-thioguanine treatment fosters cancer immune surveillance 48

6. DISCUSSION 53

7. CONCLUSIONS AND FUTURE PERSPECTIVES 57

REFERENCES 60

1. ABSTRACT

Patients affected by colorectal cancer (CRC) with microsatellite instability (MSI), which is caused by DNA mismatch repair deficiency (MMRd), are eligible for therapies based on immune checkpoint inhibitors (CPI), while microsatellite stable (MSS) tumors are not. However, a subset of MSS CRCs contains variable fractions of MMRd cells. How the presence of MMRd cells in tumors classified as MSS impacts cancer immune surveillance is largely unknown. It is also unclear whether pharmacological modulation of MMRd percentage in MMR heterogeneous tumor can occur and if this might result in the improvement of tumor immune control. To shed light on these aspects we studied isogenic mismatch repair proficient and deficient mouse tumor cells, generated by genetic inactivation of MLH1, a key component of the MMR machinery. We mixed $MLH1^{+/+}$ and $MLH1^{-/-}$ cells at different ratios, injecting the resulting heterogeneous populations in mice. In the presence of a competent immune system, the tumorigenic potential and immune surveillance of MSS/MSI ($MLH1^{+/+}$/$MLH1^{-/-}$) heterogeneous tumors was dependent upon the MMRd fraction. Tumor rejection was observed when at least 50% of the cells were MMRd, but tumor growth delay was also evident when as low as 20 % of MMRd cells were present in the mixed population and this was paralleled by immune infiltration of the tumor. Molecular profiles of samples from MSS/MSI heterogeneous tumors that evaded immune control, showed enrichment of the MSS fraction. Treatment of MSS/MSI mixed populations with the antimetabolite 6-Thioguanine (6TG) greatly enriched the MMRd fraction and improved immune response. Overall, these results suggest that genetic and/or pharmacological modulation of the DNA mismatch repair machinery can foster immune surveillance of MMR heterogeneous tumors and modulate the cancer immune environment.

2. INTRODUCTION

2.1 Microsatellite stable and microsatellite instable colorectal cancer

Colorectal cancer (CRC) represents the third most common type of tumor and accounts for more than one third of cancer-related deaths in both genders [1, 2]. Considering all stages of CRC, overall survival (OS) in patients is around 60% at 5 years from initial diagnosis, but survival rates dramatically decrease to 15% in patients with stage IV metastatic CRC (mCRC) [3, 4]. CRCs can be biologically classified into two subgroups according to microsatellite stability status, reflecting two distinct diseases with different aetiologies and alternative kind of genetic instability. Mismatch repair proficient (MMRp) tumors are defined as microsatellite stable tumors (MSS), since the length of microsatellites is stable over time. In MSS tumors, progression is driven by "chromosomal Instability", characterized by karyotypic aberrations [5]. On the other hand, in mismatch repair deficient (MMRd) tumors, defined as microsatellite instable (MSI), the advancement of the disease is promoted by Microsatellite Instability (MSI)[6], reflecting changes in the microsatellite region length during cell divisions [5]. MSS tumors represent the vast majority of CRCs, whereas MSI are approximately 15% in early stages (I-III) and only 5% in stage IV [7, 8]. MSI tumors display peculiar genetic and clinical-pathological features that differs from MSS specimens. Indeed, MSI CRCs are more frequently located in the right colon, are poorly differentiated, and have mucinous features [9]. Around 3% of CRCs, classified as MSI, arises in the context of Lynch syndrome due to germline mutations in mismatch repair (MMR) genes [9]. Alternatively, the majority of MSI CRCs are sporadic due to somatic hypermethylation of CpG islands, known as the CpG island methylator phenotype (CIMP), often targeting the promoter region of *MLH1* [10]. Furthermore, *BRAF* mutations are significantly more common in MSI rather than in MSS CRC (34% vs. 6% of cases) [11], while the incidence of APC and p53 alterations is higher in MSS then MSI tumors [12]. Importantly, MSI metastatic CRC are often resistant to common cytotoxic agents [8, 13, 14]. Interestingly, while MSS mCRCs exhibit frequently primary resistance to Immune checkpoint inhibitors (CPIs), MSI mCRCs are greatly sensitive to CPIs [2, 15-17].

2.2 Mutational characteristics of mismatch-repair-deficient cancer cell

One key mechanism to maintain genomic integrity in cells is the mismatch repair (MMR) pathway. The MMR machinery consists of several multiprotein complexes capable of detecting and correcting insertions and deletions that occur during replication processes. MutL homolog 1 (MLH1), PMS1 homolog 2 (PMS2), MutS homolog 2 (MSH2), and MutS homolog 6 (MSH6) are the key players of the MMR system and work as heterodimers to guarantee the efficacy of the entire machinery [5] (**Fig 1**).

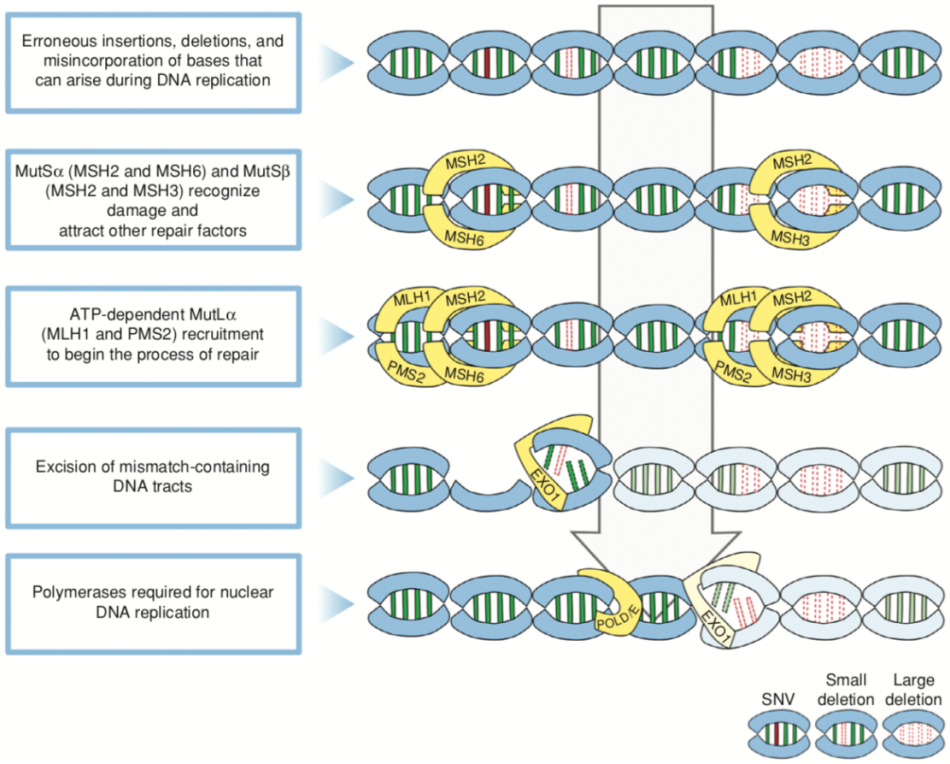

Figure 1. Mismatch repair machinery molecular players. *(from Germano et al, Cancer Discovery 2018)*

Different genetic alterations can be inherited or occur spontaneously and lead to loss of MMR function, contributing to carcinogenesis and to the emergence of MSI tumors [18]. The majority of MMRd/MSI CRCs are caused by somatic mutations in MMR genes or epigenetic downregulation of *MLH1* expression [19].

However, 3% of CRCs, classified as MSI, arises in the context of hereditary non-polyposis colorectal cancer (HNPCC), also known as Lynch Syndrome, which is a hereditary cancer syndrome characterized by heterozygous germline mutations occurring in *MLH1*, *MSH2*, *MSH6,* or *PMS2* [20]. In addition, a minimal fraction of MSI patients develop tumors due to biallelic mismatch repair deficiency syndrome (BMMR-D), which is associated with early CRC onset [21]. Specific defects in MMR allow the accumulation of specific patterns of DNA alterations. Alexandrov and colleagues demonstrated that different genetic alterations rely on the formation of peculiar mutational patterns. They performed extensive work examining 4645 whole-genome and 19,184 exome sequences, identifying 49 single-base-substitution, 11 doublet-base-substitution, 4 clustered-base-substitution, and 17 small insertion–deletion signatures [22]. As expected, also MSI tumors display exclusive mutation patterns generated by deficiency in MMR system. Indeed, the enrichment of specific nucleotide changes (C > T and T > C), double base substitution and small insertion deletion were clearly associated with MMRd tumors [22]. Importantly, distinct mutational signatures may result from different mutational processes, as shown for MMRd and Polymerase Epsilon (*POLE)*/Polymerase Delta 1 (*POLD1)* mutant tumors [2, 22-24].

2.3 CRC MMR status and immune surveillance

The genetic differences between MSS and MSI tumors greatly affect the microenvironment landscape, the evolution of cancer in terms of progression, dissemination of the tumor cells, and also response to treatments, as reported in current clinical guidelines [25, 26].

In 2016, a retrospective analysis of 1388 colorectal cancer tumors allowed for the classification of tumors in four consensus molecular sub-subtypes (CMS), based on immune cell compartments and fibroblastic and angiogenetic microenvironment [27]. The CMS1 sub-group was enriched for MSI tumors and markers of immune activation. In particular, CMS1 includes tumors harbouring high tumor mutational burden and increased neoantigen load, immune cell

infiltration (T cell, CD68+ macrophages), high levels of chemokines, but also high expression of immune checkpoint inhibitors[20, 28].

The contribution of the immune compartment in the evolution of CRC is well known, and the localization and phenotype of T-Cytotoxic, T-helper Type 1 (Th1), and T- memory infiltrating cells prominently affect survival of patients [29]. In particular, expression of genes involved in Th1 immune response correlates with a significant reduction of tumor recurrence, while cytotoxic T cell and cytotoxic molecules (Granzyme B) are enriched in tumor microenvironment of CRC patients who didn't experience tumor relapse. Accordingly, patients harbouring high density of lymphocytes, cytotoxic lymphocytes, Granzyme B and memory T cell in tumor core and invasive margin show an improved tumor free survival and overall survival [29]. Finally, Galon and colleagues proved that the immune repertoire is a reliable and independent prognostic factor in CRC [29]. Then, in 2014, the same group defined the concept of "immunoscore" as a classification criterium based on the number and localization of CD3+ and CD8+ T cell subpopulations in the tumor microenvironment, independently from MMR-status-related classification [30]. Furthermore, in 2020, the immunoscore was included in the ESMO guidelines for the staging of CRC [31]. Relevantly, in stage I-III colorectal cancer, a high immunoscore is associated with a lower risk of relapse independently from MMR status [32, 33], and similar data related to the importance of T- cell presence in tumor microenvironment have been reported for other cancer types [34, 35]. Nevertheless, a conspicuous lymphocyte infiltrate is frequently associated with MSI status in CRC [36], suggesting that the better prognosis of MSI tumors is related to the high immune infiltration [33]. Since 1994, several authors highlighted the presence of robust T cell infiltration in MSI CRC tumors, which was later confirmed by additional groups [7, 37-39](**Fig 2**). Gene expression profiles of MSS and MSI tumors revealed an augmented expression of INF-ɣ in MSI specimens, supporting an active Th1 anti-tumoral response associated with MMR deficiency [39].

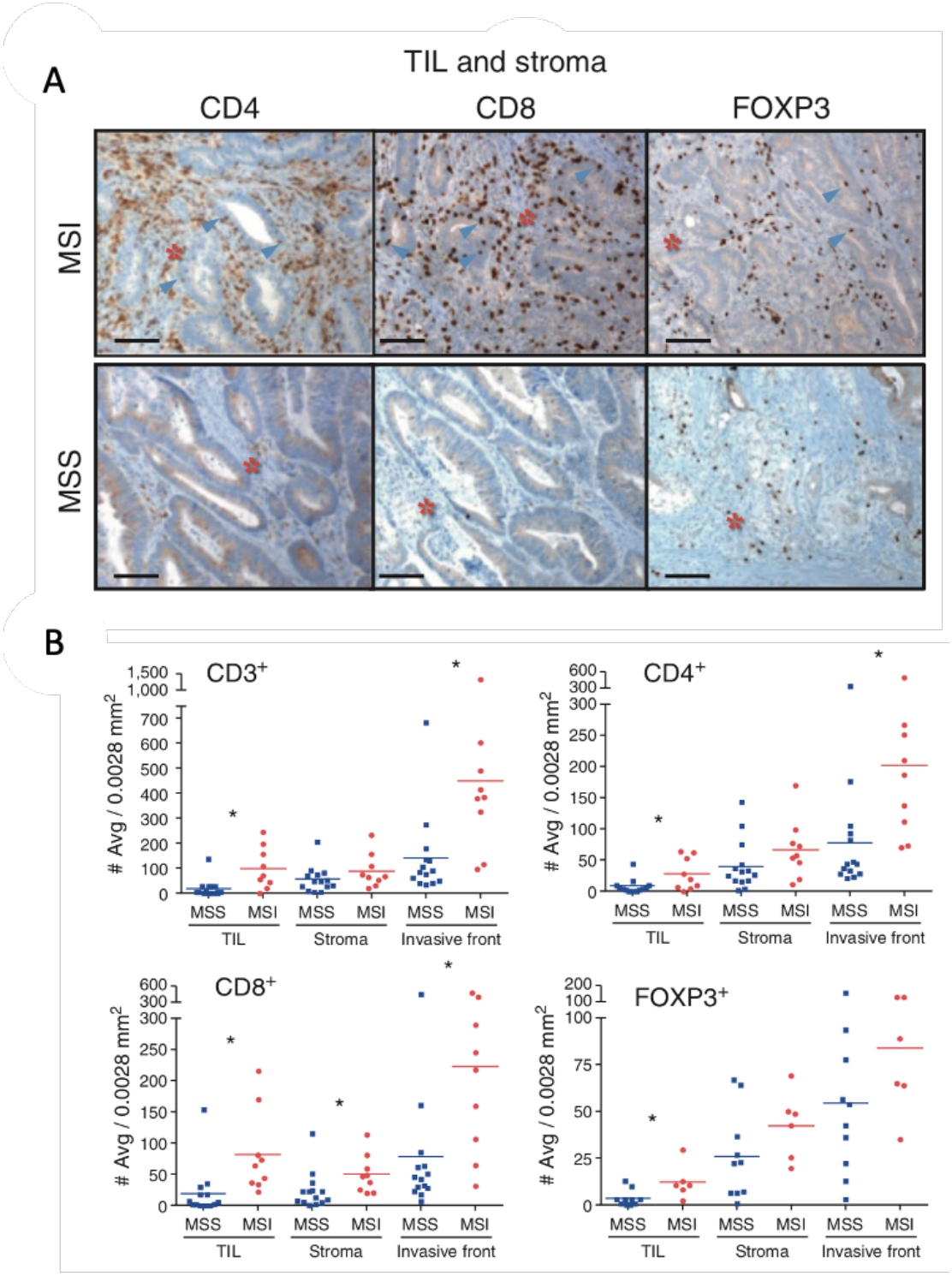

Figure 2. Differential T cell infiltration in MSS and MSI CRC. A) *Immunohistochemical staining of tumor infiltrating lymphocytes;* ***B)*** *Relative quantification (Adapted from Llosa et al, Cancer Discovery 2018)*

In addition, recent analyses performed with the CYBERSORT algorithm showed consistency with this data, observing an inflamed environment in MSI CRC tumors characterized by a prominent infiltration of M1 macrophages, CD8+ T cells, CD4+ cells, and natural killer (NK) cells [40]. Moreover, a conspicuous presence of NK cells in the CRC tumor microenvironment has been determined to be a positive prognostic factor [28].

All these data describe a dominant role of T cell response in CRC immune surveillance. Such evidence highlights the need for new criteria to stratify patients, that include the immune score, to enlarge the cohort of CRC patients to be treated with CPI therapies [41]. While the status of the anti-tumoral adaptive immune response has been extensively described during the last few years, the contribution of innate immunity in CRC needs further elucidation. Some studies reported that significant dendritic cell (DC) infiltration is associated with a better clinical outcome and correlates with the infiltration of other immune populations [42, 43]. This is expected and concordant with the fact that T cell activity strictly depends on antigen-presenting cells (APCs), which include DCs. Interestingly, Bauer and colleagues demonstrated in 2011 that S100+ dendritic cells are enriched in MSI CRC isolated from Lynch Syndrome patients [2, 44].

Summarizing, immune infiltration is considered a positive prognostic marker in CRC [29]. Importantly, a massive immune infiltration has been reported in MSI tumors [39].

Among the mechanisms that could underlie the inflamed immune environment of MSI tumors, neoantigens' role is thought to be central [45].

2.3.1 Neoantigen-dependent activation of immune surveillance in MMR-deficient colorectal cancers

MMRd/MSI CRC generate 10–50 times more tumor-specific antigens than MSS tumors [39, 46]. A functionally compromised MMR machinery leads to the accumulation of single nucleotide variants (SNVs), insertions/deletions (indels), inversions, translocations, and other structural alterations that contribute to the

mutational landscape of MMRd tumors [47]. All these alterations, if transcribed, translated, and presented by the MHC class I complex can generate new antigens (neoantigens) that, if recognized by the T cell receptor (TCR), may activate an immune response against cancer cells [48]. Notably, neoantigens are presented by MHC class I and II, triggering the activation of cytotoxic CD8+ T cells (MHC class I mediated) and the helper capacity of CD4+ T cells (MHC class II mediated) [49].

SNVs are individual nucleotide alterations that include synonymous changes (that do not affect the aminoacidic sequence of the protein) and non-synonymous changes (that alter the protein sequence). The latter include non-sense and missense mutations that lead to a different amino acidic sequence compared to the wild-type protein. These types of mutations are easy to identify using next-generation sequencing (NGS) technology. Conversely, small insertions and deletions generate frameshifts (FS), which are more challenging to detect [50]. Advanced bioinformatic tools can be used to identify and predict immune activating neoantigens by first detecting mutations or frameshifts in a specific genomic sequence followed by in silico HLA-binding analyses using sophisticated methods [51-53].

In 2017, Germano and colleagues revealed that genetic inactivation of *MLH1* in pre-clinical models led to the dynamic accumulation of mutations that triggered a robust immune response [48]. Interestingly, they noted that the response was CD8+ T-cell-dependent, and the injection of MMRd (*MLH1* KO) tumor cell lines in mice triggered increased levels of TCR rearrangements in the blood as compared to MMR-proficient tumor cells. Additional studies have underlined the importance of neoantigens in triggering T cell infiltration and in positively affecting the response to immunotherapy in several tumor types [54-56].

The concept that the number of mutations correlates with the response to CPI has been elegantly addressed by Gubin and Schreiber who introduced the idea of "winning neoantigens" [57]. They were inspired by a study from Van Allen and collaborators whereby melanoma samples with high numbers of alterations had

more chances to respond to immunotherapy due to increased odds of immunogenic neoantigens produced by tumor cells [58].

An additional key aspect to consider is the quality of alterations and how they can affect the immunogenicity of tumors. Specifically, single nucleotide changes may induce a significantly different number of neoantigens compared with frameshift mutations, most likely favouring neoantigens generated through indels. Even if a single immunogenic antigen can trigger an immune response, the number of putative neoantigens per alterations is higher if they arise from frameshifts. To test this hypothesis, the Swanton group analyzed a cohort of 5777 solid tumors across 19 cancer types from The Cancer Genome Atlas (TCGA), finding that two neoantigens could be produced from one frameshift generated by an insertion or deletion, whereas 0.64 neoantigens were achieved per SNV [18]. Interestingly, they noted that Renal Cell Carcinoma (RCC) patients had the highest number of indel mutations compared with other cancer types. Furthermore, they found CD8+ T cell signatures related to cytolytic activity in neoantigen-high RCC patients. Finally, they observed that the indel numbers were significantly associated with response to CPIs in melanoma patients. These findings demonstrated that indels generate a higher number of neoantigens than SNVs, thereby increasing the odds of neoantigen-associated immune activation and surveillance of tumor cells. Since every patient can have a peculiar mutational landscape, Leoni and collaborators analyzed 320 MSI tumor biopsies from TGCA, observing that 209 frameshift peptides were shared between patients [59]. In addition, considering an additional 20 MSI tumor patients, they identified 31 peptides in common with the initial cohort. Intriguingly, tumor specific neoepitopes derived from indel mutations have also been identified among patients with MSI endometrial, colorectal, and stomach cancers [60]. These findings pave the way to an “off-the shelf” vaccination strategy for treatment and prevention of MSI CRC tumors, although recent findings confirm that frameshift mutation frequency negatively correlates with the predicted immunogenicity due to the immune editing phenomenon [61].

The assumption that neoantigens derive from the coding region of the genome has been recently countered by the group of Perrault. Intriguingly, they proposed that in human and murine samples, almost 90% of peptides mounted on the MHC derive from non-canonical genomic sequences [62]. These findings are highly relevant in the neoantigen field and led to new hypotheses that a more extensive analysis of the non-coding portions of the genome could reveal yet undefined features of MSI tumors and potentially lead to new mechanistic knowledge and help predicting the therapeutic outcome of patients [2].

2.4 Treatment with checkpoint inhibitors in MSS and MSI mCRC patients

As previously described, in MSI CRC, the high tumor mutational burden determines neoantigen generation, resulting in a remarkable immune infiltration which is associated with a good prognosis [29, 45]. In addition, these features predispose MSI tumors to the success of CPIs [28]. Briefly, CPIs are monoclonal antibodies that targeting immune checkpoint molecules reinvigorate T cell response. Indeed, the immune checkpoint molecules are a pivotal mechanism that tumor exploits to suppress anti-tumoral response [63].

MSI CRCs display higher expression of immune checkpoints compared to MSS CRCs [39]. Notably, the introduction of CPIs dramatically changed treatment for MSI mCRC. Initially, pembrolizumab was used as an advanced metastatic line of treatment and showed an impressive 40% objective response rate (ORR) with a 90% disease control rate (DCR) in MSI mCRC patients, compared to a 0% ORR and 11% DCR in patients with MSS tumors [2, 15]. In the same setting, the combination of nivolumab plus ipilimumab achieved 55% ORR, 80% DCR, and 71% progression free survival (PFS) in 12 months [16].

The phase III randomized trial KEYNOTE-177 demonstrated the superiority of pembrolizumab over standard cytotoxic combinations +/− anti-epidermal growth factor receptor (EGFR) or anti-vascular endothelial growth factor (VEGF), the first line setting in MSI mCRC patients [64]. Notably, median progression-free survival (mPFS) in patients receiving pembrolizumab was 16.5 months versus 8.2

months among those who received cytotoxic agents (hazard ratio 0.60; 0.45–0.80) [64]. Furthermore, 83% of patients who responded to pembrolizumab were still responding at 24 months compared to only 35% of those treated with standard chemotherapy [64]. However, despite remarkable PFS and duration of response (DOR), 29.4% of patients exhibited primary resistance to pembrolizumab, compared to 12.3% of those enrolled in the standard treatment arm [64]. On the other hand, initial results from patients treated with the combination of nivolumab plus ipilimumab indicated that around 13% of MSI CRC patients exhibit primary resistance to therapy [65-67]. Further promising data from another phase III trial investigating the combination of nivolumab and ipilimumab (NCT04008030) in the same first-line setting are expected soon. In addition to the exploitation of CPIs in the metastatic setting, one trial testing the combination of short course nivolumab and ipilimumab in the neoadjuvant regimen in early-stage CRCs (NICHE trial) showed impressive pathological responses in both MMRd and MMRp CRC patients [2, 68].

Primary and acquired resistance presently limit the efficacy of CPIs in MSI mCRC patients [15, 16]; although a relevant portion of immune compartments infiltrate MSI tumors, around 30% of patients do not achieve any benefit from first-line CPIs [64]. The mechanisms of resistance and immune escape to CPIs in this subset of mCRC remain unclear [2].

2.5 Cytosolic DNA release contributes to the immunogenic properties of MMRd tumors

While the prevalent view is that the major contribution to the effectiveness of immune surveillance and CPI in MMRd cancers is linked to the number of neoantigens, recent publications have also pinpointed the contribution of cytosolic DNA in the activation of INF-mediated immune response in MSI tumors [2, 69]. The observation that activation of the immune system can also occur through other pathways such as cGAS-STING (cyclic GMP-AMP synthase–stimulator of interferon gene) is gaining traction. cGAS interacts with cytoplasmatic double strand DNA deriving from infections or cellular stress; this

is the first step of a cascade of mediators that results in the expression of genes involved in inflammatory response [70]. Data suggest that in gastrointestinal diseases, cGAS-STING activation is key for the onset of colitis and CRC [71], while in other cancer types such as prostate, accumulation of cytosolic DNA increases disease progression from non-malignant to hyperplasia to stage II [72]. Furthermore, STING activation triggers tumor growth in lung carcinoma pre-clinical models [73], most likely through interferon (INF)-mediated immune response, which has been shown to promote tumorigenesis. Finally, emerging pro-tumoral roles in metastatic processes have shown that cGAMP (cyclic guanosine monophosphate–adenosine monophosphate) can be transferred through gap junctions from tumor cells to astrocytes inducing interferon (IFN) and nuclear factor Kappa-ligand-chain-enhancer of activated B cell (Nf-kb) signaling and ultimately brain metastasis [74].

Despite these data, it has also been reported that triggering the cGAS-STING pathway regulates cellular senescence and apoptosis and enhances adaptive anti-cancer immunity [75]. Recently, the cGAS-STING pathway was implicated in initiating immune response in an IFN-dependent manner [76]. Specifically, activation of the immune system has been recently investigated, and studies have determined that DNA fragmentation induces INF response by STING, thus activating dendritic cell maturation and then CD8+ T cell activation [77]. Interestingly, stimulation of immune cells has also been described by trans-activation (tumor to immune cells). Particularly, cGAS expression by tumor cells triggers c-GAMP, which is translocated and activates STING and interferon-β production in myeloid and B cells [78, 79]. Importantly, Woo and colleagues reported the presence of cytosolic tumor DNA in dendritic cells and macrophages in vivo. They showed that activation of cGAS, STING, and interferon regulatory factor 3 (IRF3) was tumor-DNA-dependent and contributed positively to dendritic cell activation [80]. Another immune mechanism involves the recruitment and activation of cytotoxic natural killer (NK) cells [81]. Notably, the DNA damage response in a lymphoma cell line led to STING-mediated induction of retinoic acid early transcript 1 ligand (RAE1). Then, RAE1 binding natural killer group 2 member D (NKG2D) that was expressed on the NK cells led the anti-tumoral

immune response. In addition, STING activation in both tumor and immune cells may cooperate to produce different patterns of chemokines and thus induce tumor cytotoxicity by NK cells [82]. Interestingly, recent findings suggest that MMR deficiency and T-cell activation are linked by the cGAS-STING pathway [69]. Specifically, Lu and colleagues elegantly showed that in CRC and breast cancer models with defects in MMR, cytosolic DNA is accumulated and triggers a CD8+ T cell specific response. At the same time, Guan and colleagues disclosed that MLH1 regulates exonuclease 1 (EXO1) nuclease activity, and the impairment of the MLH1–EXO1 interaction leads to replication protein A (RPA) exhaustion and consequently DNA breaks and the release of nuclear DNA into the cytoplasm [83] (**Fig 3**).

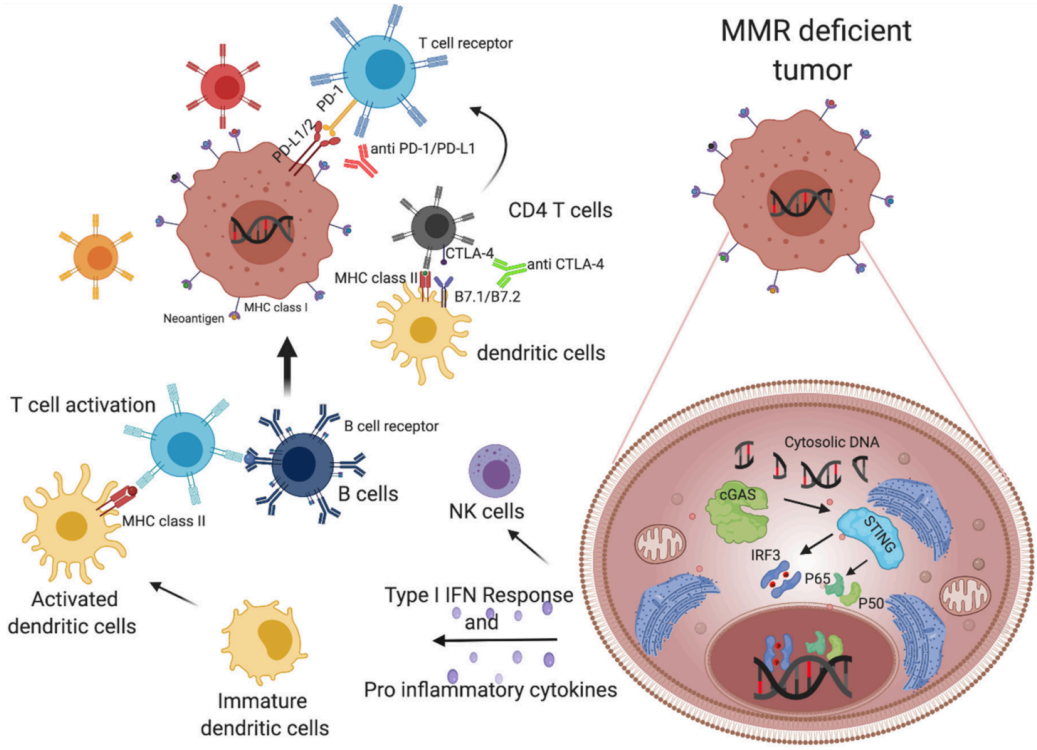

Figure 3. Cytosolic DNA and cGas-STING pathway activation triggers antigen- and INF-mediated activation of the adaptive immune system*. The contribution of neoantigens to tumor regression of MSI tumors upon CPIs has been established. However, recent findings demonstrated that cytosolic DNA accumulation occurs in MSI cancer cells [87]. As consequence of this biochemical process, the cGAS-STING pathway is activated, resulting in the induction of type I INF mediated response and*

leading to the secretion of pro-inflammatory cytokines that sustain and foster anti-tumor response through multiple mechanisms. These findings lead to emergent strategies to trigger an immune response and to enrol patients with a positive predictive response to PD-1/PD-L1 and CTLA-4.(From Amodio et al., Cancers 2021)

Overall, the cGAS-STING pathway is a promising therapeutic target in CRC. Indeed, exploiting cGAS-STING agonists could produce adjuvant effects and increase the efficacy of therapy such as radiation, vaccination, and immunotherapy [84]. These data highlight the contribution of cGAS-STING pathway, together with the MMRd-derived large number of neoantigens, to generating a productive immune response of MSI tumors once treated by immune-stimulating therapies [2].

2.6 Intra-tumoral genetic diversity of the MMR Status

Recent data highlight that MMRd and MMRp cells can coexist in the same tumor mass [85-88] (**Fig 4**).

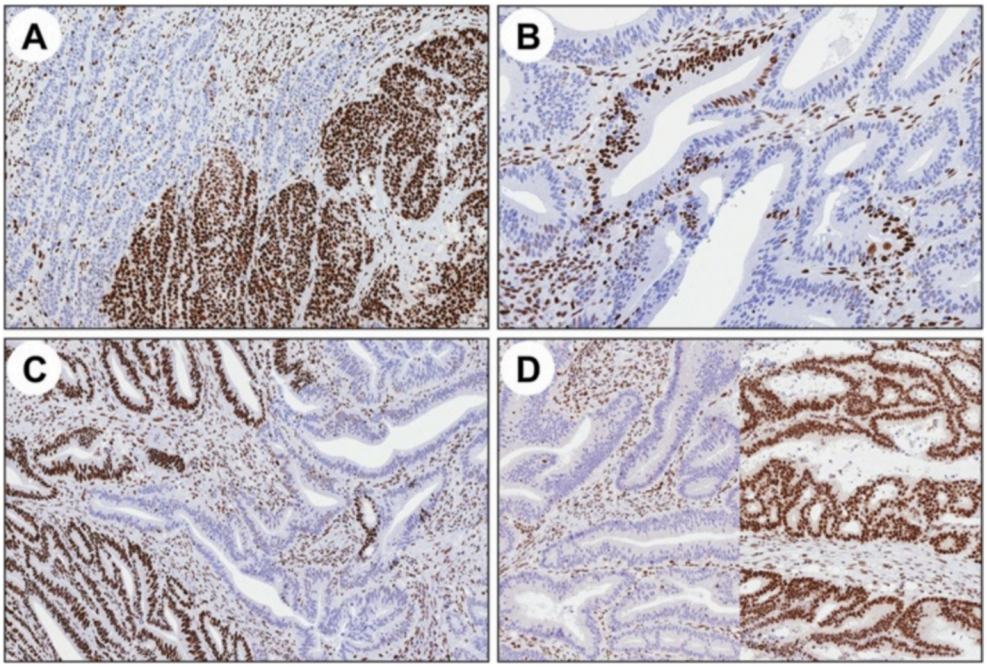

Figure 4. Examples of heterogeneous expression patterns of MMR proteins (*from Joost et al., Diagnostic Pathology 2004)*

Indeed, several atypical immunohistochemical staining displaying area of week/absent staining and area of strong positive staining have been reported in literature in the past [89-91]. Anyway, without the support of molecular evidences, heterogeneous MMR status identified in the same tumor by immunohistochemistry was often considered artefactual or a consequence of technical caveats [85]; nevertheless, the presence of heterogeneous MMR-proficient and -deficient tumors has been recently identified in a fraction of CRC patients [92, 93] To unveil potential molecular mechanism behind CRC MMR heterogeneous IHC staining patterns, Mc Charty and colleagues analysed different cases with peculiar MMR proteins expression taking advantage of histological microdissection of positive and negative area for a specific MMR marker: at molecular level, areas of proteins loss were paralleled by genetic or epigenetic alterations, oppositely from what was observed in area of retained stained. This work was one of the first evidences that different MMR components are really present in the same tumor, determining a mixed MSS/MSI cancer [85]. Following similar approaches, several other authors confirmed that MMR heterogeneity protein expression mirrors molecular patterns of MMR gene alterations [85, 86, 92, 93](**Fig 5**). Notably, also in tumors with different aetiology (breast, gastric, endometrium) similar patterns were observed, suggesting possible functional implications hidden behind the protein expression patterns [86, 88, 94]. MMR heterogeneity is considered a rare phenomenon: a retrospective quantitative analyses performed by Loupakis and colleagues reported that among unselected patients, only 0,7 % display MMR heterogeneity, a % that increase at around 6% if only MSI tumors are considered [92]. Anyway, in the era of personalized medicine, the importance of the MMR deficiency in determining therapeutic options and prognosis, imposes a deep investigation of the significance of MMR heterogeneity in clinic. Moreover, the histological diagnosis of a tumor is usually performed on a single or few tumor bioptic fragments; these are single snapshot in space and time that could fail in recapitulating a complex heterogeneous pattern, thus underestimating the real number of MMR heterogeneous patients.

Intra-lesions heterogeneity was also observed in primary and metastatic CRC tumors in a study conducted on 369 patients. In most tumors, the MSS status was

identified in both primary and metastatic specimens, whereas among 46 primary MSI tumors, nine of them were classified as MSS when the metastatic lesion was tested. Interestingly, the discrepancy was mainly limited to peritoneal and ovarian metastases [95] [2].

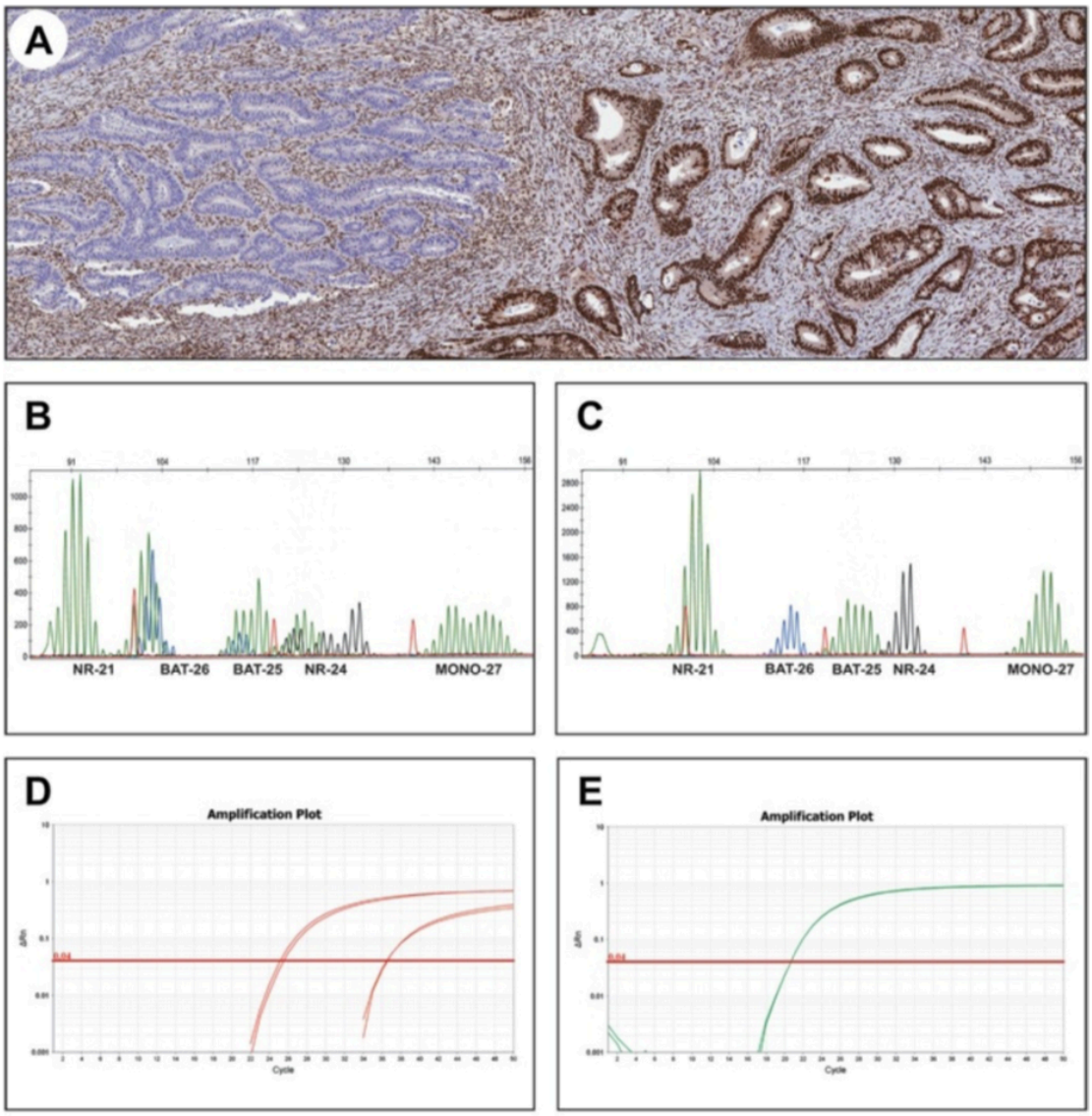

Figure 5. Heterogeneous expression patterns of MLH1 in colorectal adenocarcinoma. A) *Heterogeneous clonal loss of MLH1 staining;* ***B)*** *Microsatellite analyses corresponding to loss of staining revealed microsatellite instability;* ***C)*** *Microsatellite analyses corresponding to positive MMR protein staining revealed microsatellite stability. The differential expression is due to* ***D)*** *presence and* ***E)*** *absence of MLH1 promoter methylation, which is concordant with absent or retained staining, (adapted from Joost et al., Diagnostic Pathology 2004)*

2.7 MMR heterogeneity and immune surveillance

The implications of MMR heterogeneity in cancer progression and response to therapies are still unclear and need to be thoroughly investigated. Loupakis and colleagues described a case of a mCRC patient harbouring MMR heterogeneity at intra-tumor and inter-lesion level who experienced prolonged disease stabilization under nivolumab monotherapy and ipilimumab plus nivolumab treatment [92] (**Fig 6**). Notably, the final progression of the disease was driven by the MMRd component [92]. In contrast, Kim and colleagues observed that a heterogeneous MLH1 positivity contributed to a lack of response to pembrolizumab in a metastatic MSI gastric cancer [88]. Interestingly, primary resistance to immune checkpoint inhibitors in metastatic colorectal cancer is associated also with misdiagnosis of microsatellite instability or MMR deficient status [96]. It is conceivable that MMR heterogeneity could have crucial implication in CRC diagnosis, immune based treatment and prognosis, and accordingly should be further investigated[2].

Summarizing, heterogeneous MMR patterns exist across different cancer types, and they inevitably could affect immune surveillance. Thus, the identification of tumors that are both MMRd and MMRp could be relevant to define therapeutic strategies for MSS and MSI CRC patients.

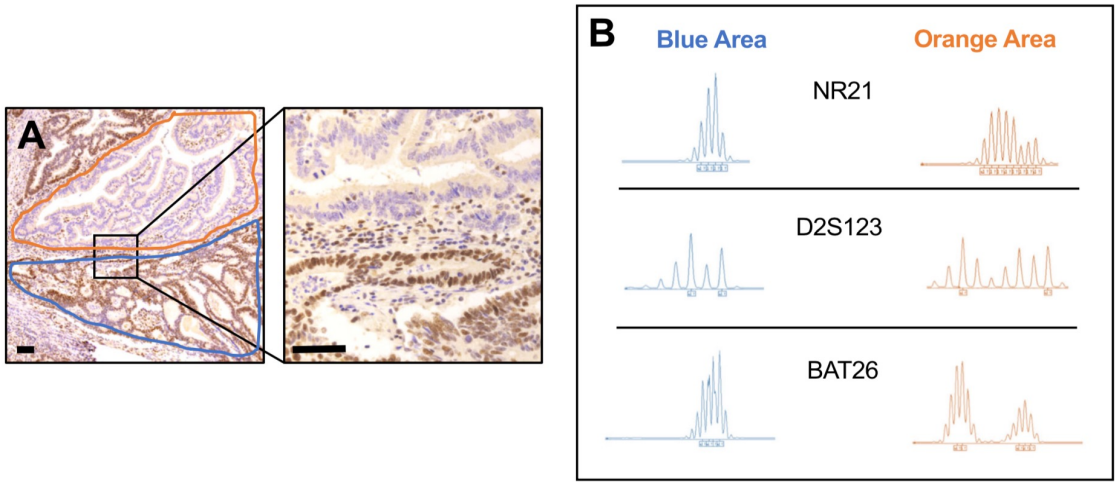

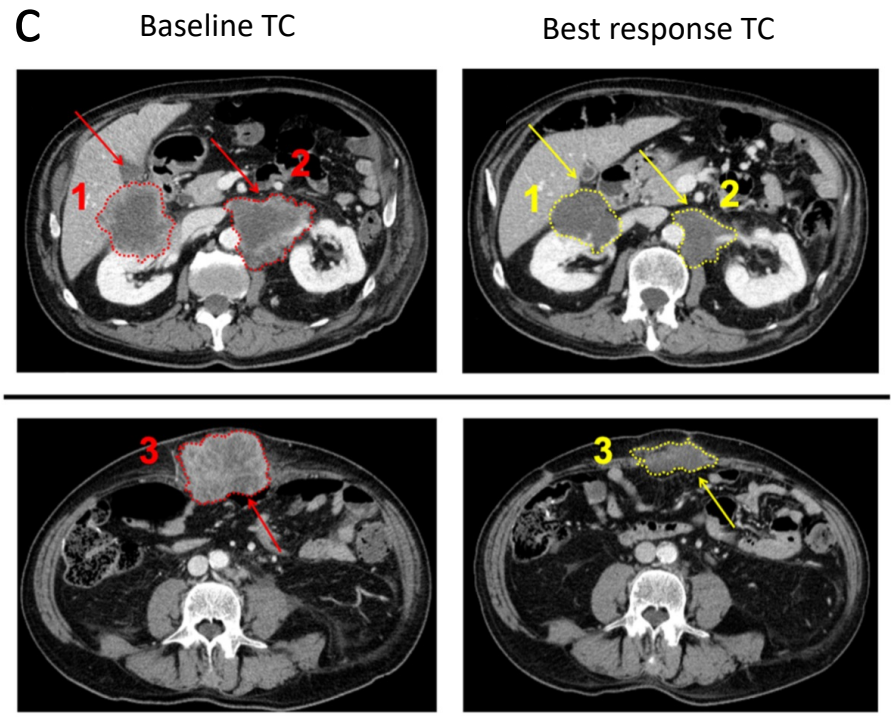

Figure 6. CRC MMR heterogeneous patient response. A) *Heterogeneous MLH1 expression in primary tumor;* ***B)*** *Microsatellite analyses of MLH1 positive and negative area revealed microsatellite stability and instability accordingly with protein expression;* ***C)*** *Baseline Computed Tomography (TC) and Best Response TC during CPIs treatment in CRC MMR heterogeneous patient lesions. (Adapted from Loupakis et al., J immunother cancer, 2018)*

2.8 Exploiting MMR heterogeneity for CRC immunotherapy

Considering the clear distinction between immune surveillance and CPIs response of MSI tumors, if compared to MSS, MMR heterogeneity might have a great impact on CRC treatment. Potentially, in MMR heterogeneous specimens two distinct immunological phenotypes co-exists: the MMRd one characterized by an inflamed and immune hot environment, the second immune-desert and refractory to immune-based therapy. How this peculiar tumor asset could elicit an immune response is unclear. It is also unclear if the modulation of the MMR heterogeneous tumor composition could favor an immune response. Interestingly, some FDA approved therapeutic agents display MMR-status dependent toxicity. It has been

previously shown that Temozolomide (TMZ), an alkylating agent approved in 2005 for first line therapy of glioblastoma [97], affects DNA repair and that prolonged exposure to this compound results in a selection of MMR deficient cells [98, 99]. Through a pharmacological drug screening on murine colon cancer MC38 and CT26 cell lines, our laboratory recently demonstrated that TMZ has preferential toxicity to MMRp cells [48] (**Fig 7**). Moreover, TMZ prolonged treatment led to the emergence of MMRd cells among MC38 parental cell population [48].

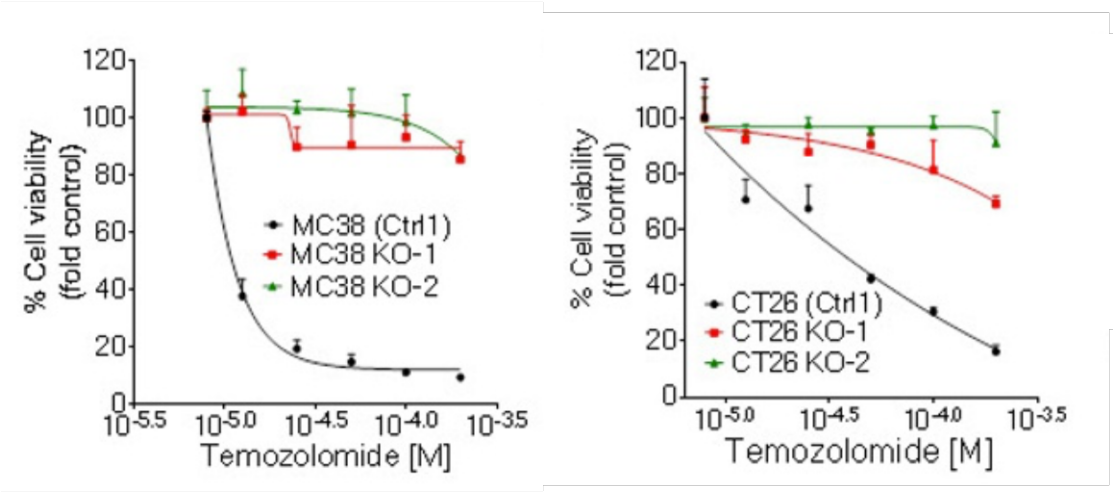

Figure 7. MLH1 dependent Temozolomide sensitivity*. Temozolomide drug screening revealed differential sensitivity of CT26 and MC38 MLH1 WT and MLH1 KO accordingly to the MMR status. (Adapted from Germano et al, Nature 2017)*

Additionally, post-treatment cells were MLH1 KO, MSI, and able to trigger immune surveillance in mice [48]. These findings were also confirmed in a large cohort of CRC human cell lines. In agreement with in vitro observations, analysis of biopsies from patients relapsing upon Temozolomide-based therapeutic regimens revealed that resistance to therapy can be driven by acquisition of mutations in MMR genes (i.e., *MSH2* or *MSH6*)[48]. In both cell lines and biopsies, MMR inactivation led to increased mutational load and higher levels of predicted neoantigens, suggesting an augmented immunogenicity. These preclinical data led us to initiate a clinical trial named ARETHUSA (NCT03519412). Within ARETHUSA, MMR-proficient CRC patient tumors are tested for MGMT expression by immunohistochemistry, and those that are negative (e.g., for MGMT promoter

methylation) are treated with Temozolomide and then tested for tumor mutational burden in post-Temozolomide tumor biopsies. Tumors with tumor mutational burden higher than 20 mutations per megabases undergo pembrolizumab treatment. This trial aims to test the hypothesis formed during preclinical studies that tumors with acquired resistance to TMZ (MMRp selectively toxic agent) might be composed mainly by MMRd cells and thereby potentially sensitive to pembrolizumab treatment [2].

Similarly, the antimetabolite 6-Thioguanine (6TG), an FDA approved chemotherapeutic agent used mainly in haematological malignancies, is known to exert differential toxicity on MMR deficient and proficient cancer cells[100, 101]

In 1998 Glaab and colleagues demonstrated that upon 5 uM 6TG exposure, MMR deficient cells displayed resistance, whereas MMRp cells were highly sensitive [101]. A functional MMR is needed to recognize the DNA-damage induced by the use of compound and to initiate the cellular response leading to cell death. In absence of a proficient MMR, 6TG induced damage is not recognized and the cytotoxic drug potential is not carried out [102, 103] (**Fig 8**). Accordingly, MSH6 deletions were identified at relapse of childhood leukemia patients upon prolonged thiopurine treatment, suggesting MMRd component enrichment ability of this class of compounds [104].

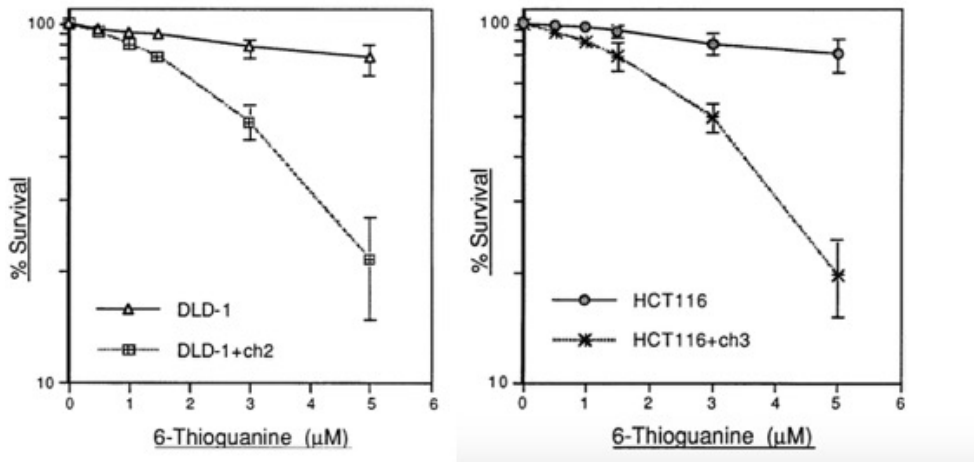

Figure 8. MMR dependent 6TG sensitivity. *6TG drug screening in CRC MSI cell lines with or without chromosome transfer harbouring functional hMSH6 (chromosome*

2-ch2) and hMLH1 (chromosome 6-ch6) that compensate intrinsic cells MMR defects. MMR function complementation confers sensitivity to 6TG (Adapted from Glaab et al., Carcinogenesis 1998)

The insensitivity of MMRd cells to 6TG and TMZ has been considered detrimental in the paste, limiting the success of chemotherapeutic regimens. Oppositely, in the context of MMR heterogeneity, in which a hot and cold tumor coexist, exploiting compounds that hamper proliferation of the MMRp component while fostering enrichment of the MMRd counterpart, could be an opportunity to reintroduce in clinic these drugs with new purposes and perspectives.

3. AIM OF THE STUDY

MSI tumors are immune infiltrated and benefit from immune based therapies. Oppositely, MSS tumors are immune desert and not eligible for immune checkpoint blockade approaches. A subset of cancers classified as MSS contains variable fractions of MMRd cells. How the presence of MMRd cells in tumors classified as MSS, impacts cancer immune surveillance is largely unknown and carries profound significance as it could have therapeutic and prognostic implications.

Our main goal is to dissect the impact of MMR heterogeneity on immune response in CRC. We are interested in understanding if the coexistence of MMRd and MMRp cells in the same cancer niche could have an impact on immune surveillance and/or immune evasion of colorectal cancer. It is also unclear whether pharmacological modulation of heterogeneous MMR populations can occur and if this might determine an improved immune control. Accordingly, we aimed at investigating whether it is possible to select MMRd cells in a heterogeneous tumor, exploiting compounds that display differential sensitivity to MMRp and MMRd cells. Subsequently, we aimed at addressing whether drug-induced MMRd enrichment might improve the outcome of CRC pre-clinical model. Overall, the final purpose of our proof-of-concept study is to investigate, from a preclinical point of view, whether MMR heterogeneity might support the extension of the fraction of CRC patients eligible for immune-based therapy

4. MATERIAL AND METHODS

4.1 Mouse cell lines

CT26 is a murine undifferentiated colon carcinoma cell line obtained from a Balb C background. CT26 were purchased by ATCC and were cultured in RPMI 1640 10% FBS, 1% glutamine and 1% penicillin/streptomycin.

Cell line was propagated three times a week to ensure the best fitness in the plate. Routinely, mycoplasma test was performed. Prior the execution of the experiments reported in this manuscript, parental cell lines were injected in the syngeneic background and the resulting tumor was exploited to re-establish in vitro a new cell culture. This procedure ensures that the models used are tumorigenic and will be not edited from the immune system of the syngeneic model in the following application. Cell were tested for mycoplasma detection regularly.

4.2 Gene editing

The knock out of the Mlh1 gene in mouse cells was generated using the genome editing one vector system (lentiCRISPR-v2) (Addgene #52961) as previously reported[48]. To reduce off-target effects, CRISPR tool http://crispr.mit.edu was deployed to design sgRNAs [48]. For these experiments, we needed transient expression of CRISPR-Cas9 system, consequently we transfected cells with lentiCRISPR-v2 vector plasmid as previously reported [48]. Transfection was performed using Opti-MEM (Invitrogen) and Lipofectamine 3000 (Lifetechnologies). After 2 days, cells were treated with puromycin (Sigma Aldrich) for 48h and then single cell dilution was performed in 6 multiple 96-well plates for each guide. The knock-out of MLH1 and the absence of Cas9 was evaluated by western blot.

The knock out of the cGAS gene in mouse cells was generated using the genome editing one vector system (lentiCRISPR-v2). The procedure was the same as the one used for MLH1.

4.3 Animal studies

All animal procedures were approved by the Ethical Commission of the University of Turin and by the Italian Ministry of Health. All in vivo experiments were executed according to institutional guidelines and international law and policies and following methods previously described [48].

We used five- to eight-weeks old female BALB/c and NOD/SCID mice purchased from Charles River (Calco, Como Italy). Each experiment was performed using at least five mice per group. For subcutaneous injection (CT26), mice were depilated, and 500 000 cells resuspended in 100ul of PBS were injected on the right flank. For abscopal experiment, 250 000 cells were simultaneously injected in 100ul PBS in both flanks.

Tumor size was measured twice a week and volume was calculated using the formula: $V = (d^2 \times D)/2$ (d = minor tumor axis; D = major tumor axis) and reported as tumor volume (mm^3, mean ± SEM of individual tumor volume). Mice were maintained in individually ventilated cages containing refinement instruments. Animal welfare was checked by veterinary personnel during all the experiments. Mice were daily monitored for social behaviours, compromised motility and sign of distress. As soon as mice fitness was impaired or tumors displayed sign of ulceration, animals were sacrificed in accordance to humane endpoint. For the experiments reported in this thesis, sample size was not predetermined using statistical methods. The investigators operated not in blind

4.4 Mice treatment

TMZ (Carbosynth) was prepared daily dissolving the powder in PBS. TMZ was administered intraperitoneally 5 days/week at 50 mg/kg. When mice started displaying signs of drug systemic toxicity, treatment was stopped, resulting in a total schedule of 2 weeks treatment. TMZ treatment was started at day 5 post injection. PBS was used as control arm.

6TG was purchased by Sellechkem and was dissolved in a stock solution of 15 mg/ml in DMSO. 6TG working solution was prepared dissolving stock solution in PBS daily. 6TG treatment concentration of 3 mg/kg was started 5 days after injection and was administered intraperitoneally daily for 5 treatments in total. DMSO treatment was used as control arm.

In both cases, mice tumor volumes were randomized before starting treatment. Mice health condition were continuously monitored by veterinary and researcher, and at first sign of distress animal were sacrificed accordingly to humane endpoint planned in the approved mice protocol.

4.5 Western Blot analyses

For western blot assays, cells were cultured in media containing 10% FBS. Proteins were extracted by lysing cell pellets in SDS buffer (50 mM Tris-HCl [pH 7.5], 150 mM NaCl, and 1% SDS). Samples were boiled at 95°C for 10 minutes and sonicated for 15-30 seconds depending on the dimension of the pellet. Eventual residual debris were pelleted by centrifugation and 5ul of supernatant were used to quantify the protein content. Quantification phase was performed using BCA Protein Assay Reagent Kit (Thermo Scientific). Detection phase was conducted with the enhanced chemiluminescence system (GE Healthcare) and peroxidase-conjugated secondary antibodies (Amersham). The primary antibodies used for this assay were: anti mMLH1 (epr3894 from AbCam), anti Actin (I-19) from Santa Cruz Biotechnology, anti-Cas9 (7A9) from GeneTex, anti-Vinculin from Millipore, anti-CGAS (D3080) from Cell signalling.

4.6 Genomic DNA extraction

Genomic DNA was extracted from SNP Frozen preserved cell pellets and SNP Frozen tumor fragments using Maxwell® Instrument (Promega) or Relia Prep gDNA tissue miniprep system (Promega). In order to achieve a realistic image about the composition of tumor content in terms of $MLH1^{-/-}$ and $MLH1^{+/+}$ cells, we extracted gDNA form the entire mass, dividing each tumor in several small pieces and then pooling together the extracted material.

4.7 Droplet digital PCR detection

Genomic DNA was amplified using ddPCR Supermix for Probes (Bio-Rad) with the murine KRAS G12D custom assay and a ddPCR Non-Homologous End Joining Genome Edit Detection assay (BioRad). ddPCR was then performed according to manufacturer's protocol, and the results were reported as the percentage or fractional abundance of mutant DNA alleles to total (mutant plus wild-type) DNA alleles. 5–10 µl of DNA template was added to 10 µl of ddPCR Supermix for Probes (Bio-Rad) and 2 µl of the primer and probe mixture. Droplets were generated using the Automated Droplet Generator (Auto-DG, Bio-Rad) where the reaction mix was added together with Droplet Generation Oil for Probes (Bio-Rad). Droplets were then transferred to a 96 well plate and then thermal cycled with the following conditions: 10 min at 95 °C, 40 cycles of 94 °C for 30 s, 55 °C for 6 min followed by 98 °C for 10 min (Ramp Rate 2 °C/s). Droplets were analysed with the QX200 Droplet Reader (Bio-Rad) for fluorescent measurement of FAM and HEX probes. Gating was performed based on positive and negative controls, and mutant populations were identified. The ddPCR data were analysed with QuantaSoft™ Analysis Pro Software (Bio-Rad) to obtain fractional abundance of the mutated DNA alleles in the wild-type or normal background. The quantification of the target molecule was presented as number of total copies (mutant plus WT / edited plus unedited) per sample in each reaction. Fractional Abundance is calculated as follows: F.A. % = (Nmut/(Nmut + Nwt)) × 100) for KRAS G12D assay (where Nmut is the number of mutant events and Nwt is the number of WT events per reaction) or FA %=, NHEJ edited alleles/(wild-type + NHEJ edited alleles), in other words, edited alleles/total alleles (edited + unedited).

To precisely determine the MLH1 content of each tumor, three independent sampling were performed and analysed.

4.8 In vitro enrichment assay

CT26 MLH1$^{+/+}$ MLH1$^{-/-}$ mixed populations were plated in 6 Multiwell plates (100 000 cell/well) at day 0. After 24h cells were treated in vitro with DMSO, 6-Thioguanine 1 uM or Temozolomide 200uM (day 0). At two different time points, day 4 and day 7-8, cells were detached, pelleted and gDNA was extracted. MLH1$^{-/-}$ cells percentage was evaluated throughout droplet digital PCR assays as previously reported. For the second timepoint, all cells were split (1:10) at day 4. Three technical and biological replicates were performed for each condition.

4.9 Immunophenotyping

Whole tumors were explanted and dissociated with Tumor dissociation Kit from Miltenyi biotechnology. After a first step of mechanical smashing with Gentle Macs Dissociation Kit, tumors were enzymatically digested for 30 minutes at 37°C. Flow cytometry analyses were performed using the FACS Dako instrument Cyan. Immune staining was performed using the following antibodies purchased by Biolegend: PerCp anti-mouse CD45 (30F11), FITC anti-mouse CD4 (RM4-5), PE anti-mouse CD8a (YTS156.7.7), APC anti-human/mouse CD11b (M1/70), Mouse LIVE/DEAD Fixable Viability Stain 780.

4.10 Statistics

GraphPad Prism software was used to perform statistical analyses. For in vitro experiments, statistical differences were calculated using Two Way ANOVA (multiple comparison). For in vivo experiment, statistical significance for tumor growth was evaluated using non-parametric test (p values were adjusted with Mann-Whitney correction). The number of animals for in vivo experiments were calculated according to requirements from the Italian Ministry of Health. Animal studies were conducted in accordance with international law and policies and institutional guidelines.

5. RESULTS

We hypothesized that the presence of MMRd/MSI cells can prompt an otherwise MMRp/MSS tumor to be recognized and controlled by immune surveillance. To understand how intra-tumoral heterogeneity in MMR status influences activation of the immune system and to systematically assess its therapeutic relevance we developed mouse cancer models recapitulating the MMRp/MMRd heterogeneity found in clinical specimens. The hosting lab previously used genome editing to generate colorectal (CT26), pancreatic (PDAC) and breast cancer (TSA) cells lacking the Mlh1 gene ($MLH1^{-/-}$)[48]. We mixed $MLH1^{+/+}$ and $MLH1^{-/-}$ cells at different ratios, injecting the resulting heterogeneous populations in mice. Clones used to perform the mixing experiments are listed in (**Fig 9**).

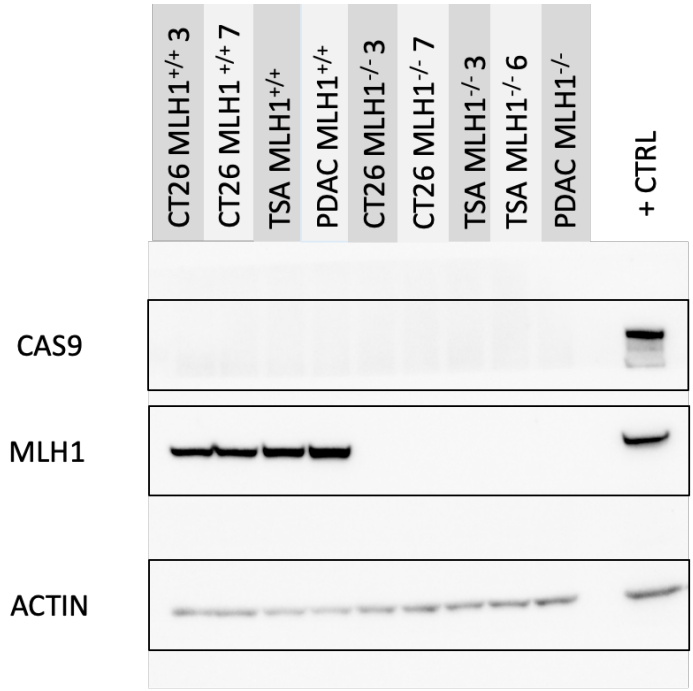

Figure 9. MLH1 and CAS 9 protein expression evaluated by Western Blot. *CT26, TSA and PDAC clones were tested for the expression of MLH1 and CAS9 by Western Blot. Actin was used as loading control.*

$MLH1^{-/-}$ cells display MSI status, increased mutational burdens and higher levels of predicted neoantigens[48]. They grow poorly when injected in syngeneic mouse models and when they generate tumors, these are remarkably sensitive to

CPIs therapy [48]. To begin understanding whether and how intra-tumoral molecular heterogeneity influences immune system activation we created a spectrum of MMR heterogeneous CT26 populations combining MMRp and MMRd isogenic cells at different ratios. In particular, to recapitulate possible scenario of MMR heterogeneity found in human tumors, different proportions (20/80, 50/50, 80/20) of MLH1$^{+/+}$ and MLH1$^{-/-}$ cells were mixed, while homogeneous populations composed entirely of MLH1$^{+/+}$ and MLH1$^{-/-}$ cells served as controls (**Fig 10**).

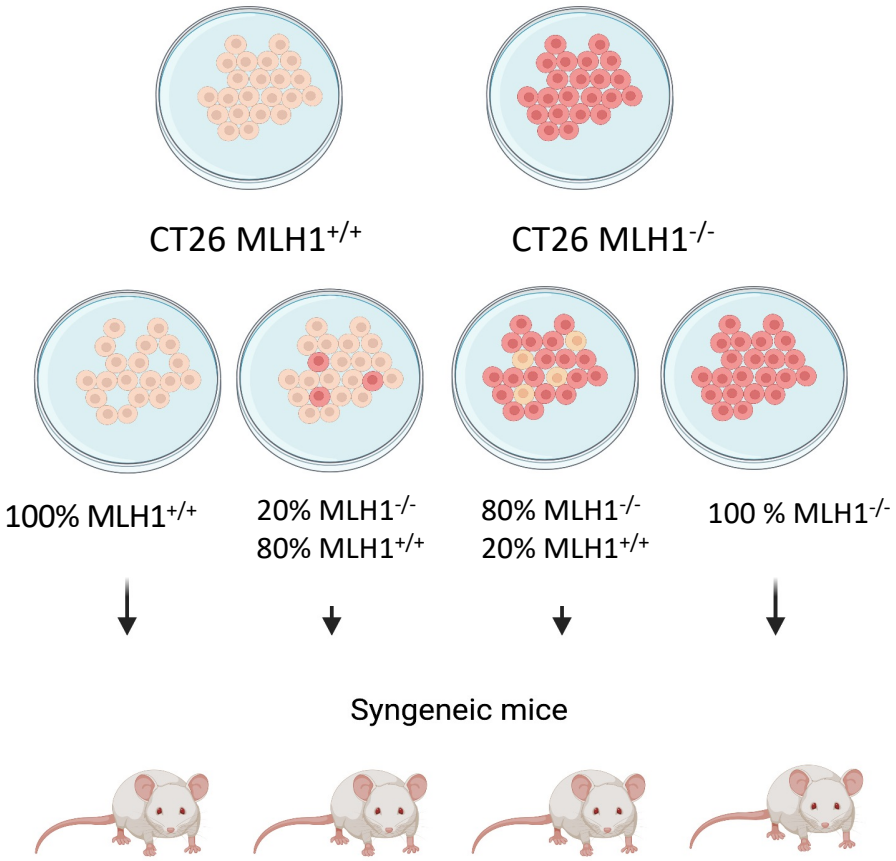

Figure 10. Schematic representation of CT26 mixing experiment

For these assays, we used a highly immunogenic MLH1$^{-/-}$ cell model lacking tumorigenic potential when injected in syngeneic mice owing to the accumulation of genomic alterations over time. To facilitate molecular profiling, droplet digital

PCR (ddPCR) probes were designed to selectively detect MLH1$^{+/+}$ and MLH1$^{-/-}$ variants in gDNA extracted from the mixed populations.

5.1 The MMRd component affects the growth of MMRd/MMRp heterogenous tumors

Tumor populations with molecular heterogeneity in MMR status were injected in syngeneic mice and tumor growth was monitored over time (**Fig 11**). We found that tumor growth delay was broadly proportional to the fraction of MMRd CRC cells present in the heterogeneous tumor (**Fig 11 A**).

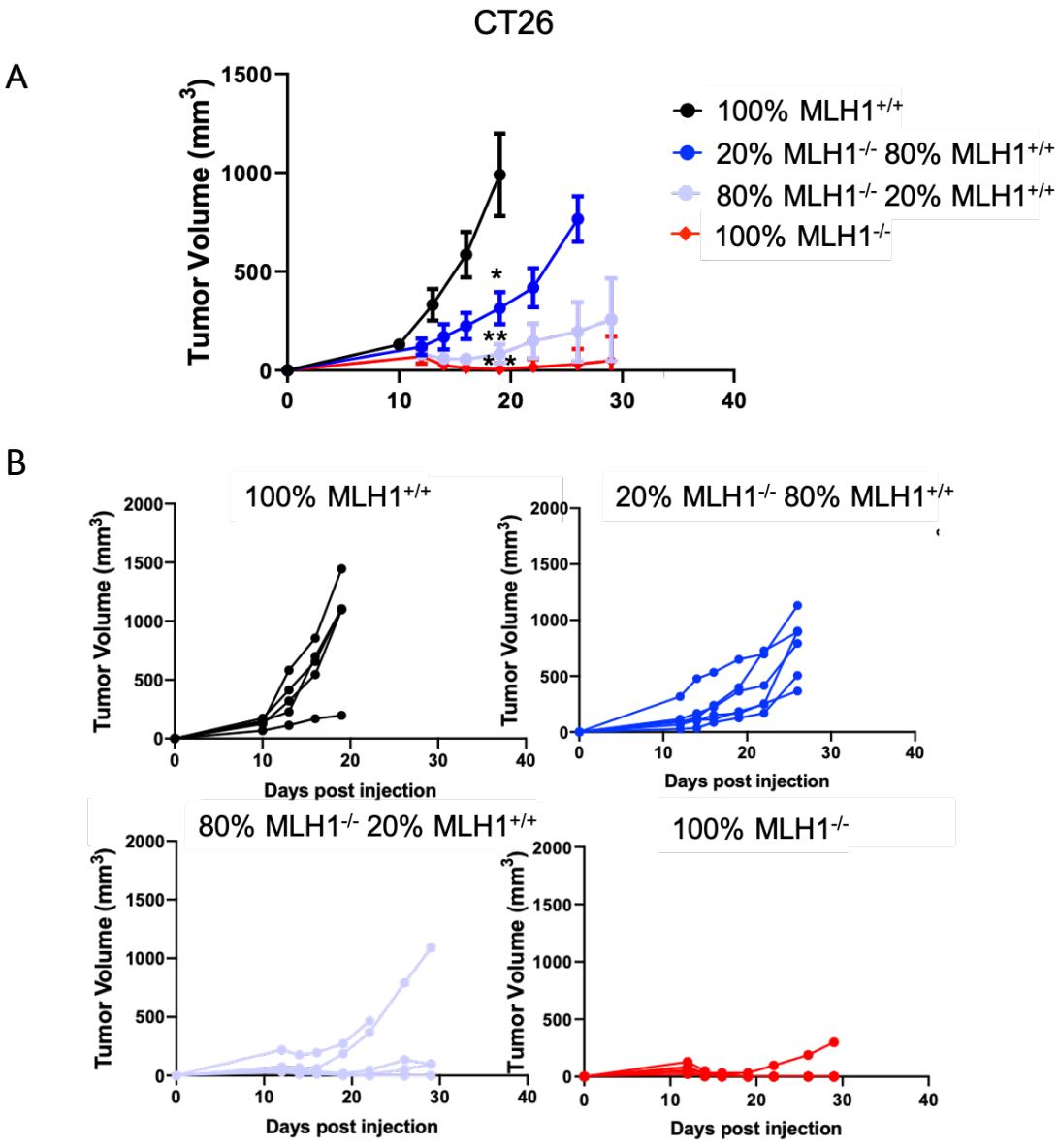

Figure 11. MMR heterogeneity affects tumor growth in CT26 mouse model. A) *CT26 cell populations (100% MLH1$^{+/+}$, 100% MLH1$^{-/-}$, 20% MLH1$^{-/-}$ 80% MLH$^{+/+}$, 80% MLH1$^{-/-}$ 20% MLH1$^{+/+}$) were subcutaneously injected in immunocompetent mice Balb C (5 x 10^5 cells per mouse). Tumor growth was monitored two times per week and reported in the graph as average of mice tumor volumes (mm^3) ± SEM. MLH1 mixed tumors display tumor growth delay dependent upon the MLH1$^{-/-}$ fraction;* ***B)*** *Tumor volume of single mice was represented. Each experimental group was composed at least of 5 animals. Statistical significance was evaluated by Mann-Whitney test: *p<0,05; **p<0,01*

The presence of 20% of MMR deficient cells was sufficient to delay tumor growth in mice, possibly indicating that the MSI fraction had a bystander effect on the MSS component. Accordingly, a fraction of the animals injected with a population harbouring 80% of MMRd cells was unable to develop a palpable tumor, suggesting that a small MSS component in an MSI tumor does not always lead to a tumorigenic phenotype (**Fig 11 B**). Notably, also a lower fraction of MMRd cells (50%) impairs tumor growth as compared to a 100% MLH1$^{+/+}$ tumor (**Fig 12 A, B**).

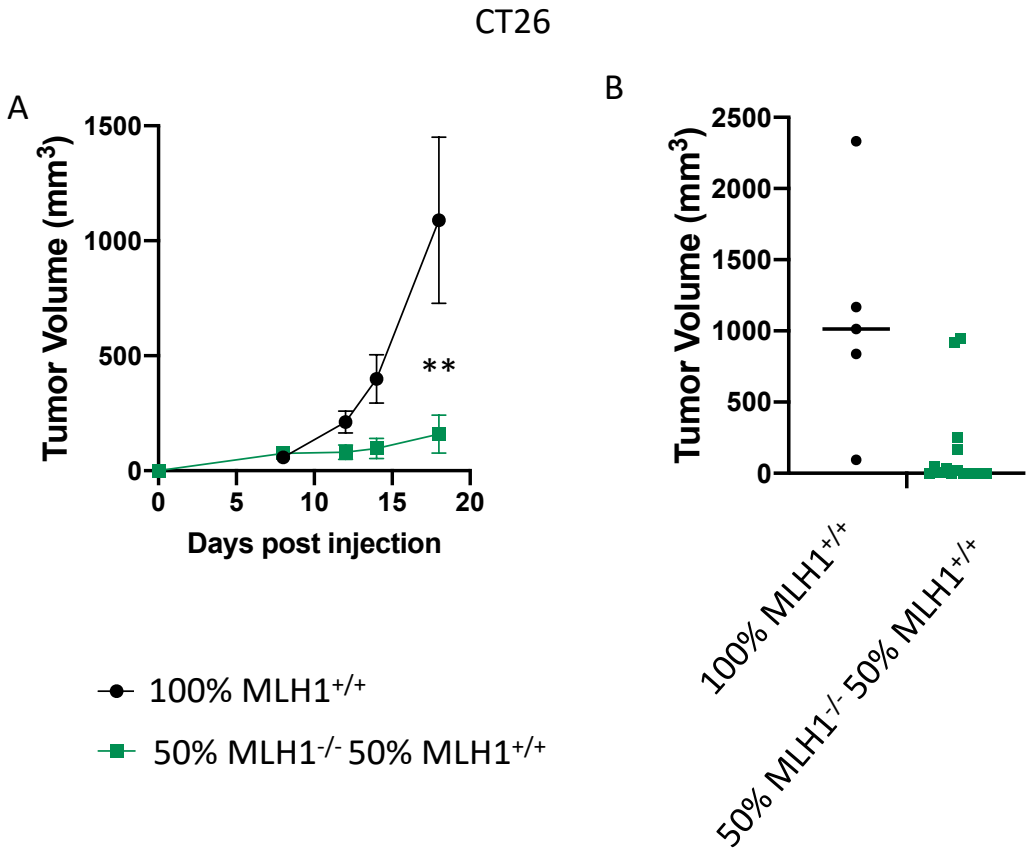

Figure 12. MMR heterogeneity impairs CT26 tumor estabilishment in immunocompetent mice . A) *50% MLH1 $^{-/-}$ 50% MLH1 $^{+/+}$ and 100% MLH1 $^{+/+}$ CT26 cell populations were subcutaneously injected in immunocompetent mice (5 x 10^5 cells per mouse). Tumor growth was monitored two times per week and reported in the graph as average of mice tumor volumes (mm^3) ± SEM.* ***B)*** *Tumor volume of single mice at day 18 is reported. Each experimental group was composed at least of 6 animals. Statistical significance was evaluated by Mann-Whitney test:* ** p = 0,005

5.2 Tumor growth delay is immune driven in MMR heterogeneous CT26

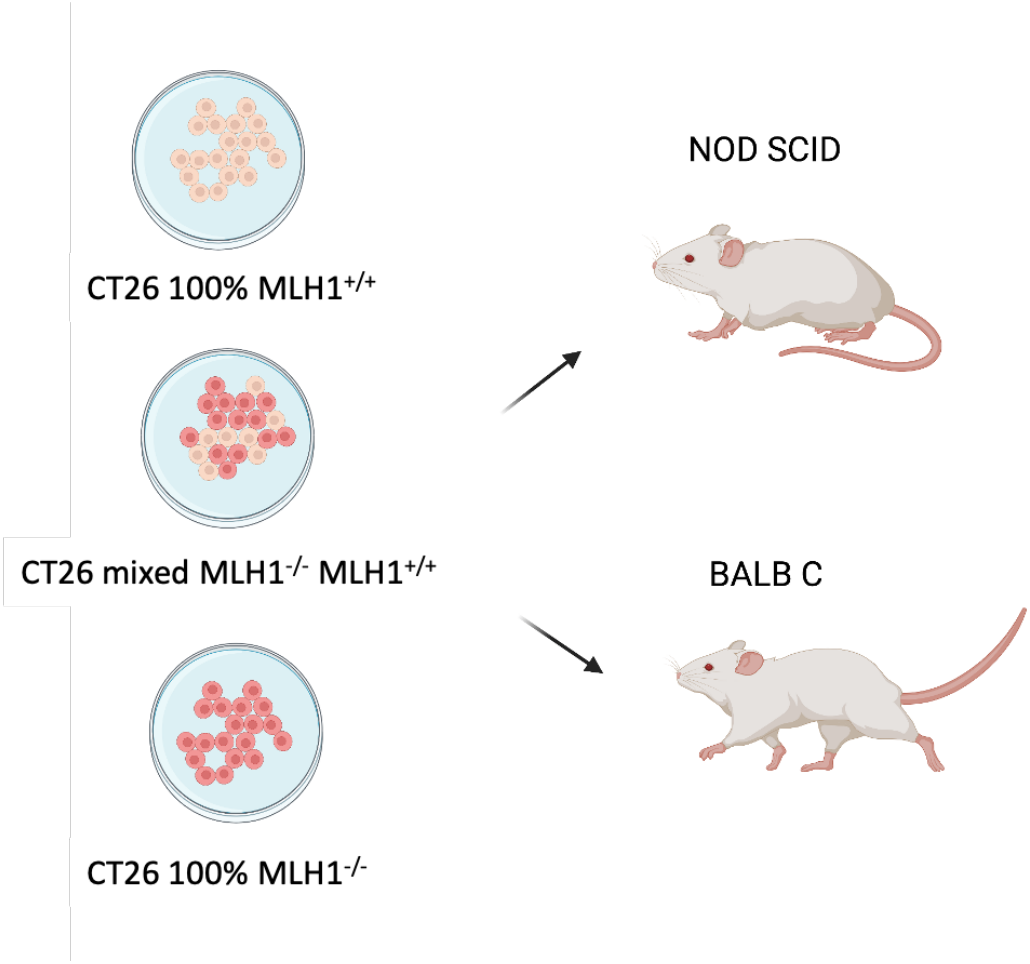

Figure 13. Schematic rappresentation of mixing experiment performed parallely in immunocompetent and immunocompromised mice

To assess whether the tumor growth delay observed in MLH1 heterogeneous population was immune mediated, we performed parallel injections of $MLH1^{-/-}$/ $MLH1^{+/+}$ heterogeneous populations (0/100, 50/50, 80/20, 100/0) in immunocompetent (Balb C) and immunocompromised (NODSCID) mice (**Fig 13**).

Independently from the MSI/MSS ratio all heterogeneous populations were able to engraft and rapidly expand in NODSCID mice, leading to ethics sacrifice in less than 3 weeks. On the contrary, when injected in immunocompetent animals, tumor growth delay or tumor rejection was observed, thus confirming results of experiments in **fig 11** and **fig 12** (**Fig 14**). Notably, in all conditions in which as low as 50% of cells were MMRd, when mixed populations were injected in immunocompetent animals, a fraction of mice rejected completely the tumor (**Fig 11, Fig 12, Fig 14**)

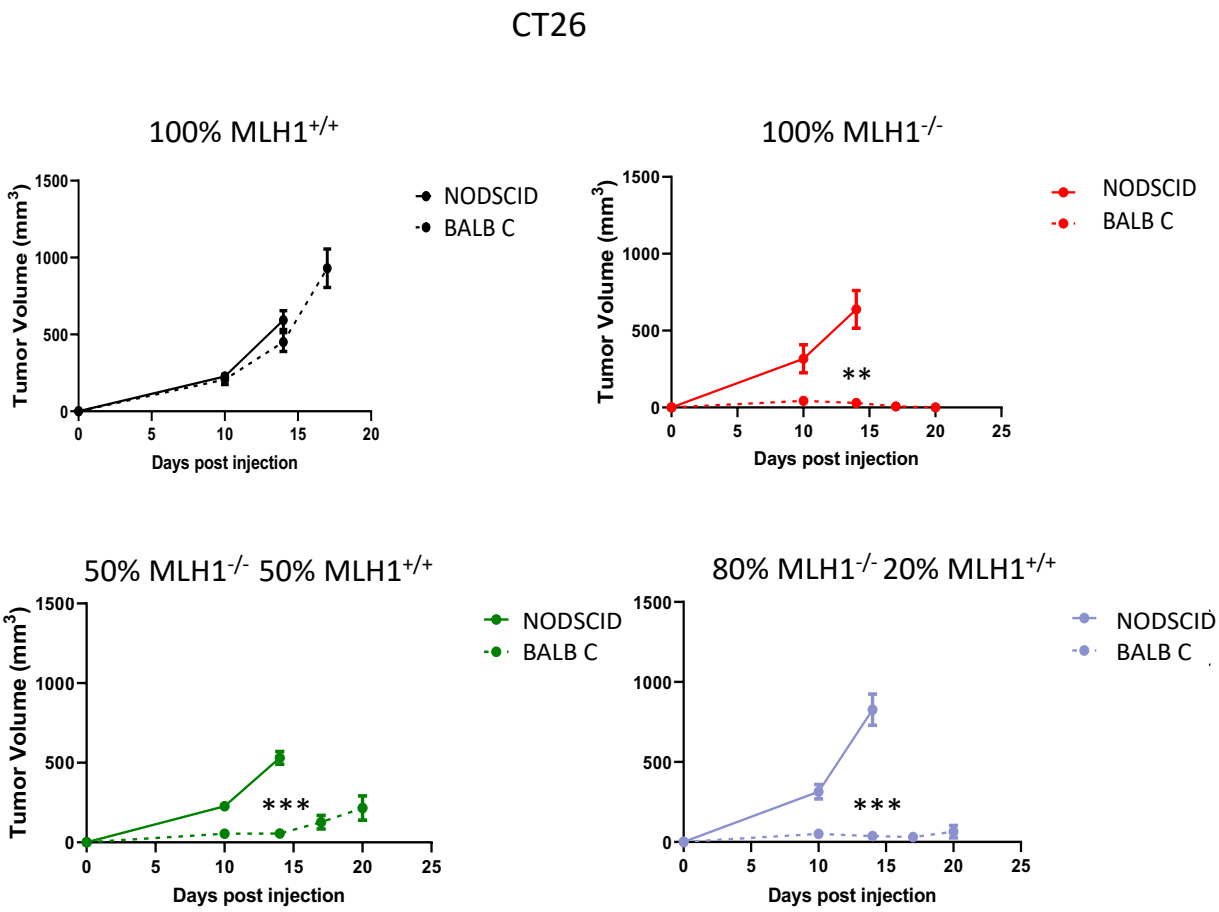

Figure 14. MMR heterogeneity impairs tumor growth exclusively in immunocompetent animals. *MLH1 $^{-/-}$/MLH1 $^{+/+}$ CT26 mixed population (0/100, 50/50, 80/20, 100/0) were injected simultaneously in immunocompetent Balb C mice and immunocompromised NODSCID mice (5 x 10^5 cells per mouse). The average tumor volumes ± SEM are reported. Each experimental group was composed at least of 6 animals. Statistical significance was evaluated by Mann-Whitney test:* **p<0,005, ***p=0,0001.

5.3 Modulation of the local tumor immune microenvironment by MMR deficient cells is key for immune surveillance.

Different processes could underlie reactivity of the immune system triggered by MMRd cells. These include increased antigenicity and immunogenicity through modulation of neoantigen profiles, increased tumor mutational burden or the activation of the INF response via the cGAS-STING pathway [45, 69]. Results in Fig. 11 and 12 show that a subset of mice injected with MMRd/MMRp mixed populations harbouring a small fraction of MMRp cells does not develop tumors. We wondered which processes could underlie the reactivity of the immune system against the MMRd cellular fraction and hypothesized that cellular or soluble factors controlled by MMRd cells could target the MMRp fraction (a form of "bystander effect"). To begin mechanistically define these aspects, we performed an "abscopal" experiment by injecting 100% MLH1$^{+/+}$ and 100% MLH1$^{-/-}$ populations simultaneously in the opposite flanks of mice. Specifically, we inoculated 250 000 MLH1$^{+/+}$ and 250 000 MLH1$^{-/-}$ cells in the two flanks of a group of mice, and monitored if the growth of each mass was influenced by the composition of the population injected contralaterally (**Fig 15 A**). As shown in (**Fig 15 B, Fig 15 C)**, the MLH1$^{+/+}$ tumor growth was not influenced by the presence of a MLH1 $^{-/-}$ mass in the opposite flank. Indeed, growth rates of MHL1$^{+/+}$ tumor in mice injected simultaneously with MLH1$^{-/-}$ cells in the opposite flanks was comparable with that of a MLH1$^{+/+}$ mass in the presence of a contralateral MLH1$^{+/+}$ tumor (**Fig 15 C**)

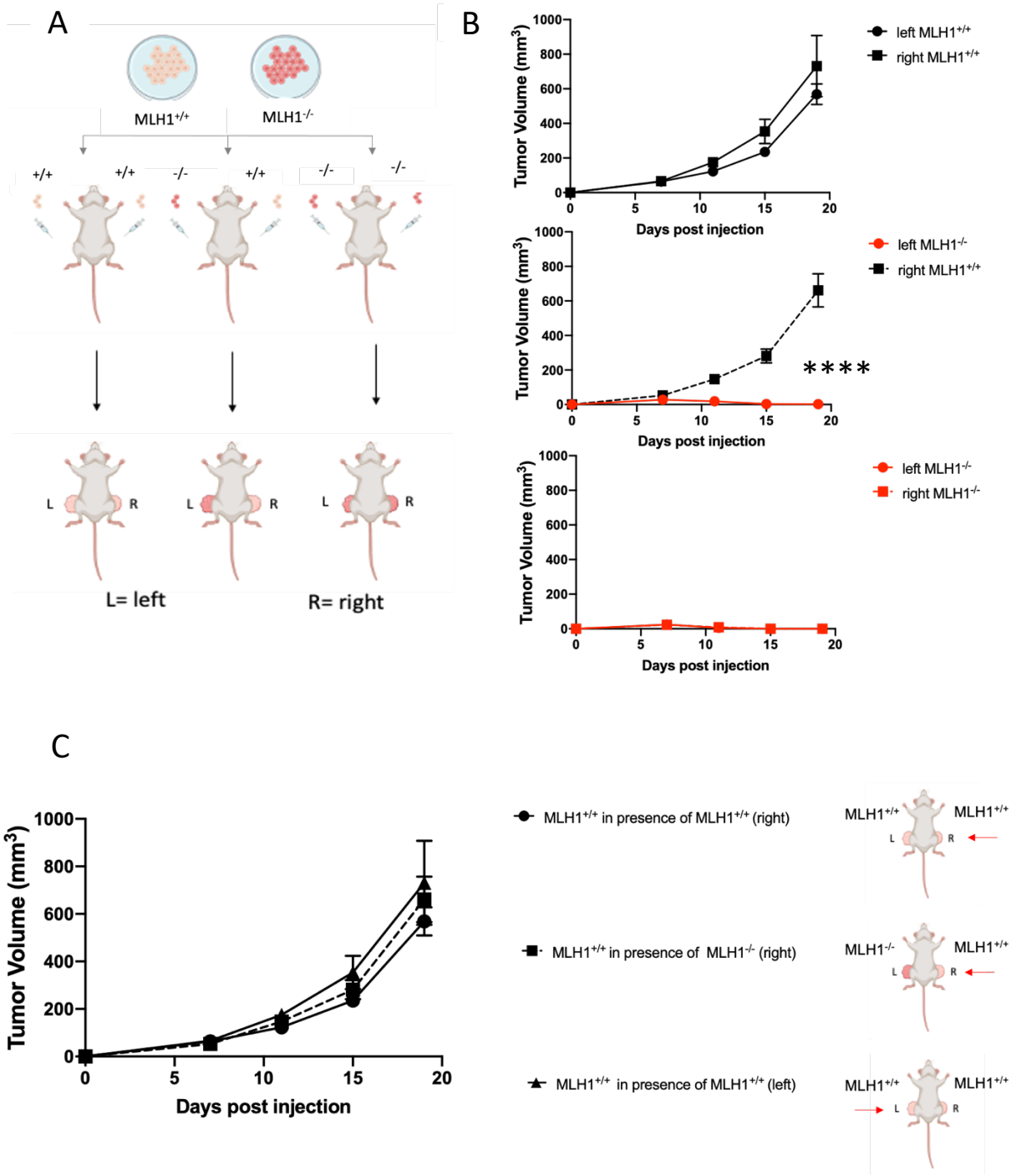

Figure 15. Abscopal experiment: simultaneous injection of MMRp and MMRd tumors in contralateral flanks of mice. A) *Graphical summary: 100 % MLH1$^{+/+}$ and 100% MLH1$^{-/-}$ CT26 cells were simultaneously injected in two flanks of the same animal. Different combinations were studied (left MLH1$^{+/+}$right MLH1$^{+/+}$; left MLH1$^{-/-}$right MLH1$^{-/-}$; left MLH1$^{-/-}$ right MLH1$^{+/+}$). A total of 2,5 x 10^{5} cells were injected in each flank to parallel the amount (per mouse) used in the other experiments;* ***B)*** *MLH1$^{+/+}$ cells were tumorigenic and resulted in tumor growth over time, while*

MLH1$^{-/-}$ tumors were edited. Tumor growth was monitored two times per week and reported in the graph as average of mice tumor volumes ± SEM. ***C)*** *Comparison between MLH1$^{+/+}$ tumors growth (in presence of MLH1$^{+/+}$ or MLH1$^{-/-}$ tumor in the opposite flank) is reported in the graph. Each experimental group was composed at least of 12 animals. Statistical significance was evaluated by Mann-Whitney test:* ****p<0,0001. *L= left, R= right*

This experimental approach suggests that the local tumor microenvironment (driven by MMRd cells) is necessary to trigger an immune response against the MMRp component.

5.4 Profiling the immunological milieu of MMR heterogeneous tumor

We studied whether the presence of a MLH1$^{-/-}$ component was sufficient to increase immune infiltration in MMRd/MMRp heterogeneous tumor. To address this question, we injected different proportions of MLH1$^{+/+}$/MLH1$^{-/-}$ CT26 cells (20%-80%, 50%-50%, 80%-20%) in immunocompetent mice. Tumors were monitored daily and when tumor volume started to stabilize (day 11), they were explanted and subjected to immunophenotypic characterization. Specifically, we assessed infiltration of CD8+ T and CD4+ T cells.

As previously reported, tumors composed of 100% MLH1$^{-/-}$ cells displayed a substantial CD8+ immune infiltration as compared to their 100% MLH1$^{+/+}$ counterpart (**Fig 16**). Tumors formed by MMRp/MMRd variable fractions displayed increased number of CD8+ T cell as compared to the 100% MLH1$^{+/+}$ controls. Of note, tumors containing as little as 20% of MLH1$^{-/-}$ cells displayed levels of CD8+ cells comparable to those composed only of MLH1$^{-/-}$ cells (**Fig 16B**). These data suggest that the presence of a small portion of MMRd cells is able to modulate tumor microenvironment increasing infiltration of the cytotoxic compartment. Furthermore, even if phenotypically the immune surveillance of these heterogeneous is not explicit, the presence of a hot immune milieu could be therapeutically relevant.

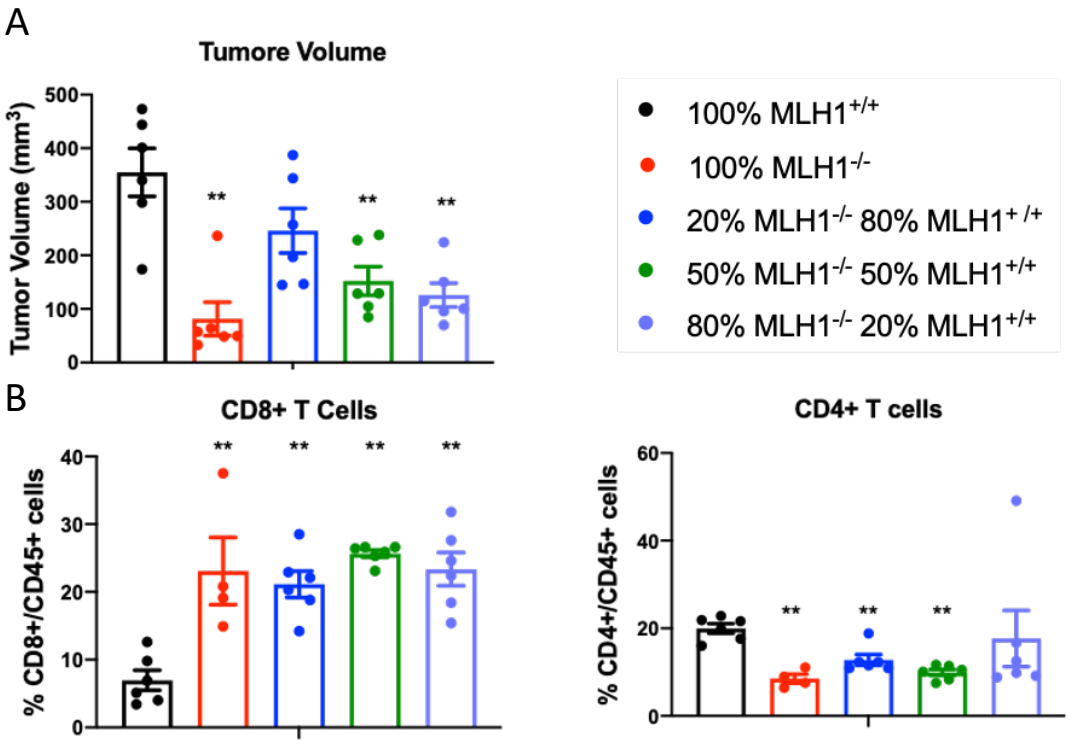

Figure 16. The MMRd fraction modulates the immune environment of MMR heterogeneous tumors. A) *MMR heterogeneous CT26 populations (100% MLH1$^{+/+}$, 100% MLH1$^{-/-}$, 20% MLH1$^{-/-}$ 80% MLH1$^{+/+}$, 50% MLH1$^{-/-}$ 50% MLH1$^{+/+}$, 80% MLH1$^{-/-}$ 20% MLH1$^{+/+}$) were injected in immunocompetent mice (5 x 10^{5} per mouse). After 11 days, mice were sacrificed and tumors were recovered and processed for immunological analyses. The tumor volume at day 11 is reported.* ***B)*** *Immune infiltrate was evaluated by cytofluorimetry. T cells (CD4+ and CD8+) were evaluated. CD4+ and CD8+ T cell were gated within CD45+ alive cells. Statistical significance was evaluated by Mann-Whitney test:* **p<0,005

5.5 Immune escape of MMR heterogeneous tumors is driven by the MMR proficient fraction

As discussed above, the presence of the MMRd component in heterogeneous tumors initiates immune surveillance which, in some instances, leads to complete tumor rejection, however in a fraction of the mice tumors escape from the immune control and rapidly progress leading to sacrifice for ethical reasons (**Fig 11**, **Fig 12, Fig 14**). We wondered what could lead to reduced immune control and eventually to cancer outgrowth. To address this, tumors which "escaped" and

grew despite any immune surveillance, as reported in Fig 14, were explanted and genomic DNA was extracted (**Fig 17A**). To specifically determine the MLH1$^{+/+}$ and MLH1$^{-/-}$ fractions a droplet digital PCR assay was designed and deployed (**Table 1**).

Sample	Target	Positive events	Negative events	Fractional Abundance (%)
CT26 100 % MLH1$^{+/+}$ A	MLH1 WT	2080	15997	100
	MLH1 KO	0	15997	0
CT26 100 % MLH1$^{+/+}$ B	MLH1 WT	1168	17739	100
	MLH1 KO	0	17739	0
CT26 100 % MLH1$^{+/+}$ C	MLH1 WT	396	7810	100
	MLH1 KO	0	7810	0
CT26 100 % MLH1$^{-/-}$ A	MLH1 WT	0	18791	0
	MLH1 KO	811	17980	100
CT26 100 % MLH1$^{-/-}$ B	MLH1 WT	0	16946	0
	MLH1 KO	657	16289	100
CT26 100 % MLH1$^{-/-}$ C	MLH1 WT	0	20177	0
	MLH1 KO	685	19492	100
NEG CTRL	MLH1 WT	570	17553	100
	MLH1 KO	2	17551	0
POS CTRL	MLH1 WT	0	17503	0
	MLH1 KO	623	16880	100
water	MLH1 WT	0	18011	0
	MLH1 KO	0	18011	0

Table 1 . Droplet ditigital PCR specificity for MLH1$^{+/+}$ and MLH1$^{-/-}$ detection . *gDNA from 100% MLH1 $^{+/+}$ and 100 % MLH1$^{-/-}$ CT26 cells were analyzed throughout ddPCR to test assay specificity. MLH1$^{-/-}$ positive control (POS CTRL), MLH1$^{-/-}$ negative control (NEG CTRL) and water were used as technical control. Each sample was measured three times (A,B,C). Positive and negative events for each target gene (MLH1 WT and MLH1 KO) were measured as indicated in material and methods of the thesis. Fractional abundance was calculated as % of MLH1$^{+/+}$ and MLH1$^{-/-}$ cells*

Analyses of escaped samples revealed that the tumors which eventually grew were composed mainly of MLH1$^{+/+}$ cells (**Fig 17 B**). Furthermore, in all samples, the MMRp component present at the end of the experiment increased as compared to the pre injection samples. Moreover, in a fraction of the specimens MLH1$^{-/-}$ cells were completely lost and the samples were almost completely constituted of MMRp cells. These data suggest that MMR heterogeneity could underlie a new mechanism of immune evasion and prompts the generation of a therapeutic

strategy aimed to target the MMRp component to increase MMR heterogeneous tumor immune surveillance.

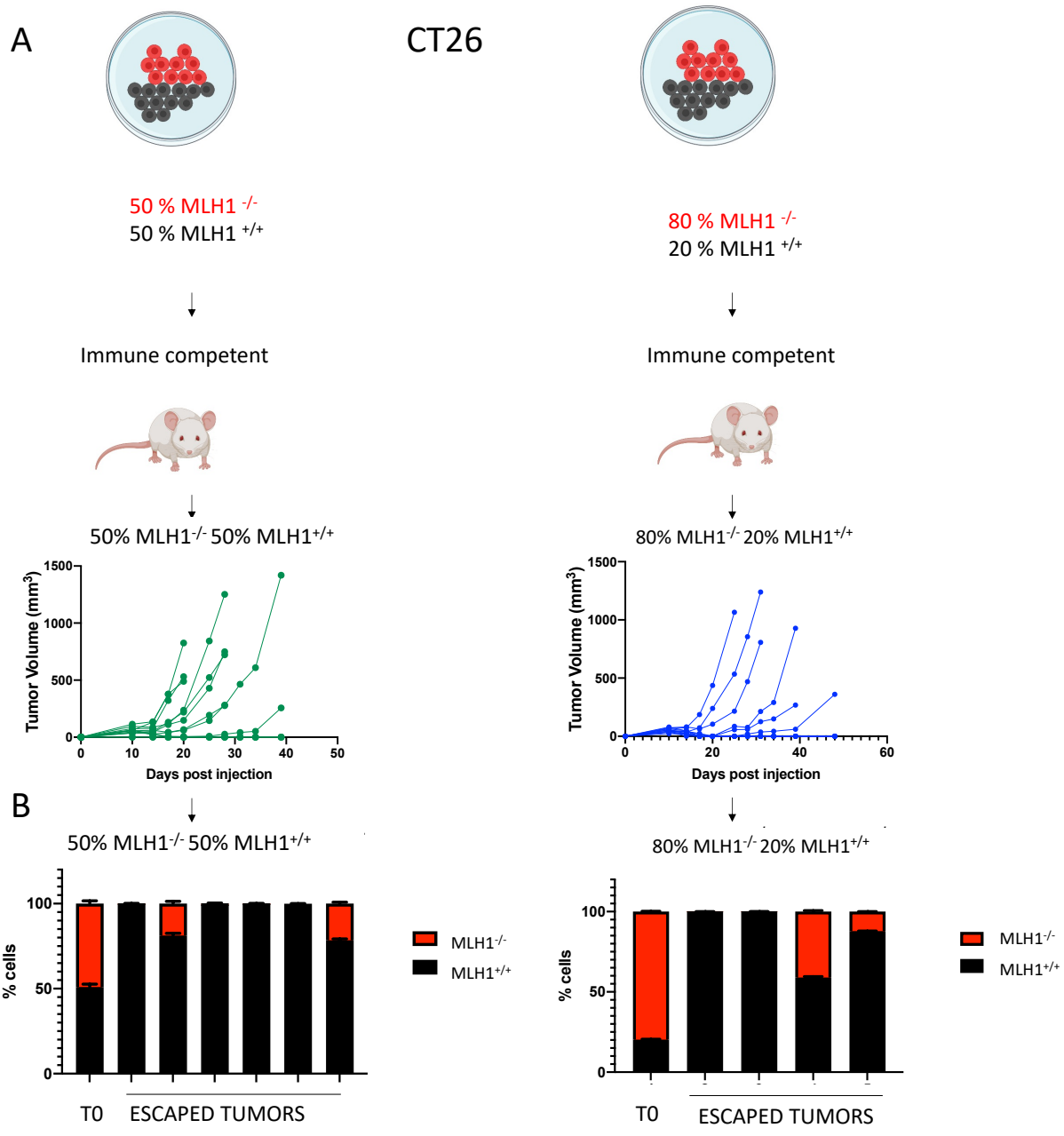

Figure 17. The MMRp fraction drives immune evasion of MMR heterogeneous tumor in immunocompetent mice*. Tumor escaped from immune control during the experiment reported in fig 14 were analyzed at molecular level.* ***A)*** *50% MLH1$^{-/-}$ 50% MLH1$^{+/+}$ and 80% MLH1$^{-/-}$ 20% MLH1$^{+/+}$ CT26 cell populations were subcutaneously injected in immunocompetent mice (5 x 10^5 cells per mouse). Tumor*

growth was monitored two times per week and reported in the graph as single mice volume (mm^3) Each experimental group was composed of 12 animals. ***B)*** *DNA from day 0 cell population (injection day) and from the whole outgrown tumors was extracted. gDNAs were exploited to evaluate $MLH1^{-/-}$ and $MLH1^{+/+}$ cell fraction throughout ddPCR analyses. Results are reported in the bar graph. T0 represents the $MLH1^{+/+}$ $MLH1^{-/-}$ cells percentage of mixed population at day 0. "Escaped tumors" indicate the $MLH1^{+/+}$ $MLH1^{-/-}$ cells percentage of tumors explanted after immune evasion.*

5.6 6-thioguanine and Temozolomide treatments of MMR heterogeneous tumors enriche for the MMRd deficient component and improve immune surveillance

A small fraction of MMRd cells is able to establish an augmented immune surveillance compared to a MMRp tumor, but is not enough to determine tumor elimination (**Fig 11**). Moreover, MMR heterogeneous tumors that were able to evade immune control revealed an increase of the MMRp component (8). We reasoned whether it would be possible to boost immune surveillance and limit MMR heterogeneous tumor recurrence by enriching the MMRd component of the tumor cell population. We and others have previously shown that exposure to the alkylating agent TMZ and 6TG can result in the selection of MMRd cells [48, 101].

We reasoned that those compounds could be used to select/enrich for MMRd fractions in heterogeneous populations of cancer cells. We therefore treated CT26 20% $MLH1^{-/-}$ 80% $MLH1^{+/+}$ cells with both agents and analysed the composition of the surviving populations at different timepoints. We found that, as soon as 72-96hr after drug exposure, there was a substantial increase of the MMRd component as compared to the MMRp one (**Fig 18 A**). Encouraged by these results the experiment was repeated by diluting a very small fraction (1%) of $MLH1^{-/-}$ in $MLH1^{+/+}$ cells. Upon 6TG selection, there was a remarkable reversal of the population composition which over a period of 8 days became mostly composed of $MLH1^{-/-}$ cells (**Fig 18 B**). These results suggest that pharmacological intervention can modify the composition of tumors with molecular heterogeneity of the MMR status.

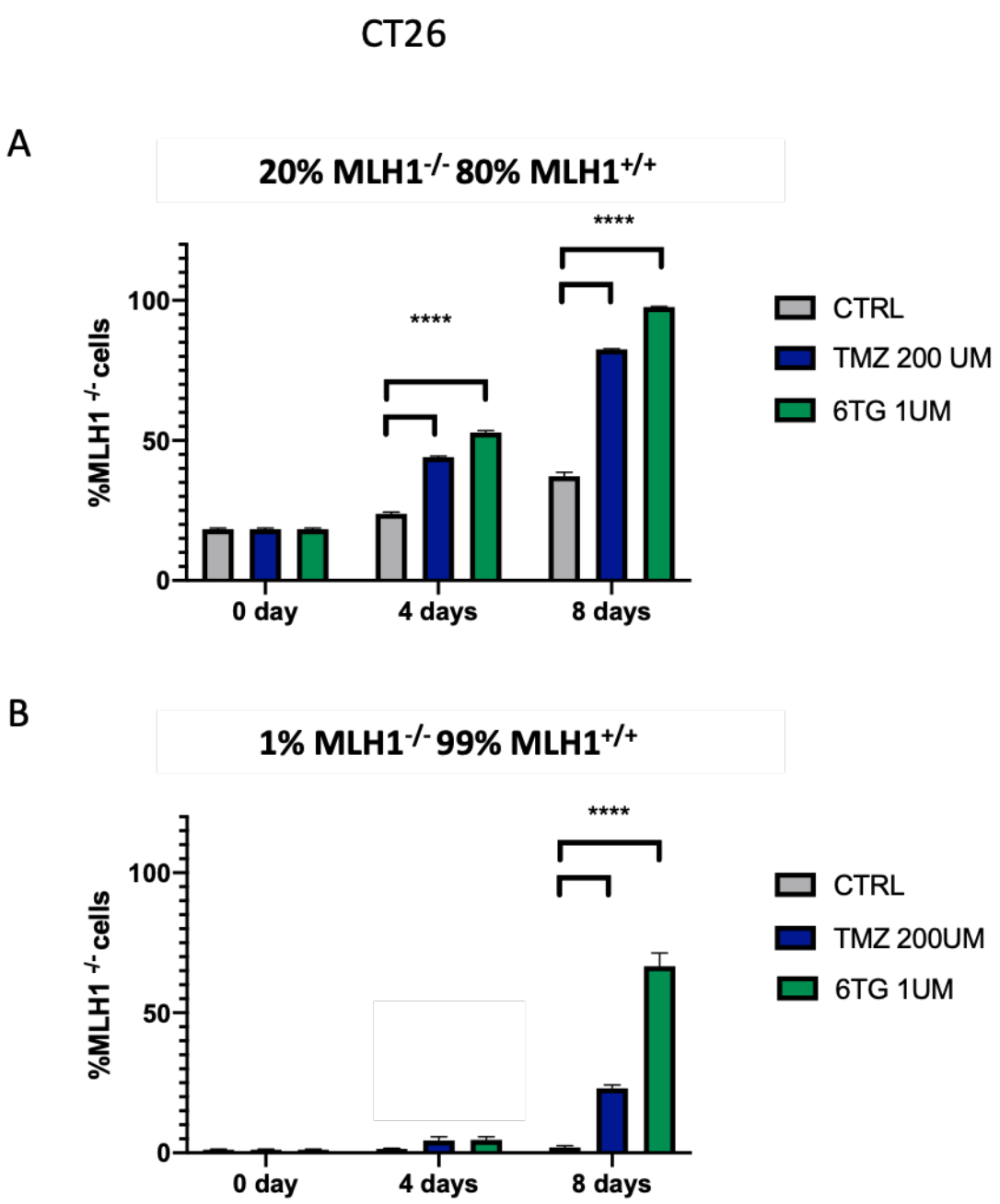

Figure 18. Treatments with 6-Thioguanine and Temozolomide increase MMRd component in heterogeneous tumors. ***A*** *CT26 20% MLH1$^{-/-}$ 80% MLH1$^{+/+}$ and* ***B*** *1 % MLH1$^{-/-}$ 99% MLH1$^{+/+}$ cells were plated in a six multiwells (1 x 10^{5} per well). After 24h, cells were treated with TMZ 200uM, 6TG 1uM or DMSO. At 1st time point, after 4days, cells for each condition were pelleted and used for gDNA extraction; simultaneously, a parallel plate was passaged 1:10 and kept in culture until day 8 under drug treatment. At day 8, cells of the second time point were pelleted and gDNA was extracted. gDNA deriving from each timepoint was exploited to perform ddPCR analyses. 6TG and TMZ increased the MLH1$^{-/-}$ content overtime compared to the t0 composition. Experiment was performed three times, and each condition was performed in technical triplicates. This figure reports one out of three representative*

experiments. Twoway ANOVA (multiple comparison) was used for statistical analyses: **** p<0,0001

We asked whether pharmacologically driven MMRd cells enrichment could improve immune surveillance. We therefore treated a mixture of CT26 cells (20% $MLH1^{-/-}$ 80 % $MLH1^{+/+}$) with 6TG or TMZ for 10 days and injected the resulting population in immunocompetent mice. In parallel, we performed ddPCR analyses to determine the composition of the injected cell populations (**Fig 19 A, B**). As expected, treated mice presented a strong increase of the $MLH1^{-/-}$ fraction in the cells prepared for inoculation (**Fig 19 B**). Strikingly, when injected in immunocompetent mice, 6TG treated and TMZ treated cell populations formed small tumor masses or did not grow at all in immunocompetent mice (**Fig 19 C, D**). To confirm that this effect was immune driven and not related to the effect of drug treatment on the target cells, the experiment was performed in parallel in immunocompromised animals. 6TG and TMZ *in vitro* treatments only modestly hindered tumor growth of cell mixtures injected in NODSCID mice, reflecting the expected (cell autonomous) effect of two anticancer agents (**Fig 19 C**). Differently from what observed in immunocompetent mice, all tumors grew in immune deficient animals (**Fig 19 D**). These data suggest that 6TG- and TMZ-induced enrichment of MMRd component can be exploited to maximize immune surveillance.

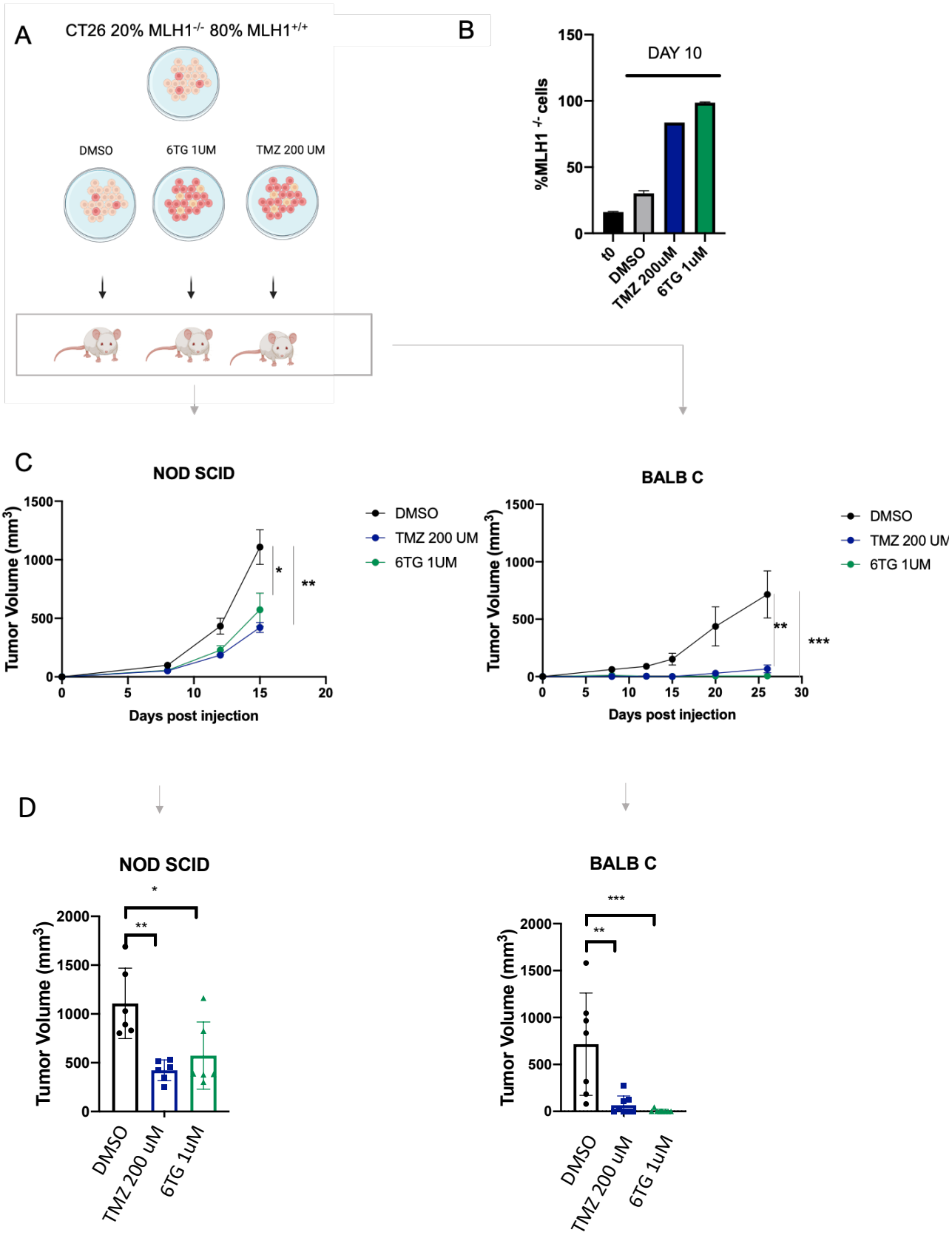
A
CT26 20% MLH1-/- 80% MLH1+/+
DMSO
6TG 1UM
TMZ 200 UM
B
DAY 10
%MLH1 -/- cells
150
100
50
0
t0
DMSO
TMZ 200uM
6TG 1uM
C
NOD SCID
Tumor Volume (mm3)
1500
1000
500
0
0
5
10
15
20
Days post injection
DMSO
TMZ 200 UM
6TG 1UM
*
**
BALB C
Tumor Volume (mm3)
1500
1000
500
0
0
5
10
15
20
25
30
Days post injection
DMSO
TMZ 200 UM
6TG 1UM
**
***
D
NOD SCID
Tumor Volume (mm3)
2000
1500
1000
500
0
*
**
DMSO
TMZ 200 uM
6TG 1uM
BALB C
Tumor Volume (mm3)
2000
1500
1000
500
0
***
**
DMSO
TMZ 200 uM
6TG 1uM

Figure 19. In vitro pharmacological selection of MMRd cells increases immune surveillance. A) *Experimental scheme: CT26 (20% MLH1$^{-/-}$ 80% MLH1$^{+/+}$) cells were plated in 10 cm dishes (1 x 10^5). After 24h, drug selection (6TG 1uM, TMZ 200UM or DMSO) were applied for 10 days.* ***B)*** *At day 10, cells were detached, gDNA was extracted and analysed for the MLH1$^{-/-}$ content throughout ddPCR. In parallel, 5 x 10^5 cells resulting from the in vitro treatments phase were injected in NODSCID and Balb C mice.* ***C)****, Tumor growth was monitored two times per week and reported in the graph as average of mice tumor volumes ± SEM;* ***D)*** *Single mice tumor volumes at day 15 (NODSCID) and 26 (Balb C) is reported. The number of tumor free Balb C at day 26 is: 0/8 for DMSO, 4/8 for TMZ, 7/8 for 6TG. Each experimental group was composed at least of 6 animals. Statistical significance was evaluated by Mann-Whitney test:* *p<0,05, **p<0,005, *** p<0,0005

5.7 In vivo 6-thioguanine treatment fosters cancer immune surveillance

We next assessed the impact of 6TG and TMZ treatment in vivo. For this reason, we tested the efficacy of the two compounds against syngeneic implants of cell mixtures with variable proportions of MMR proficient and MMR deficient cells. (**Fig 20A**)

A

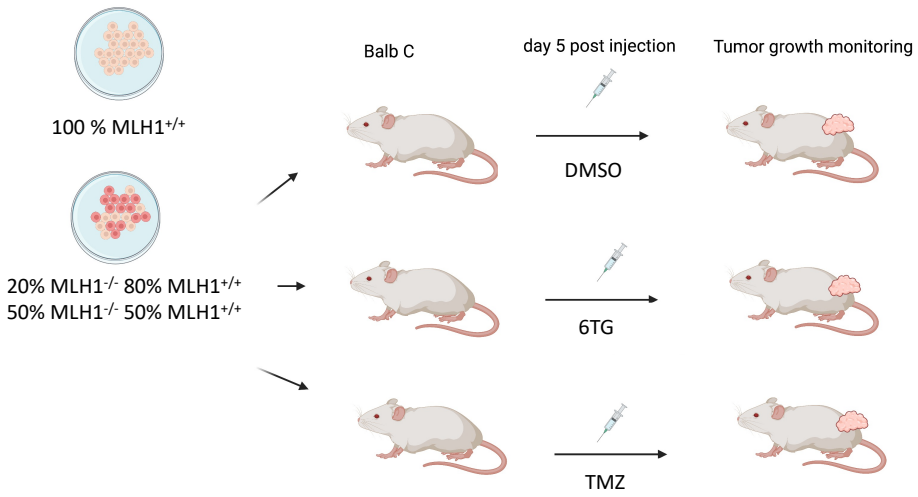

B

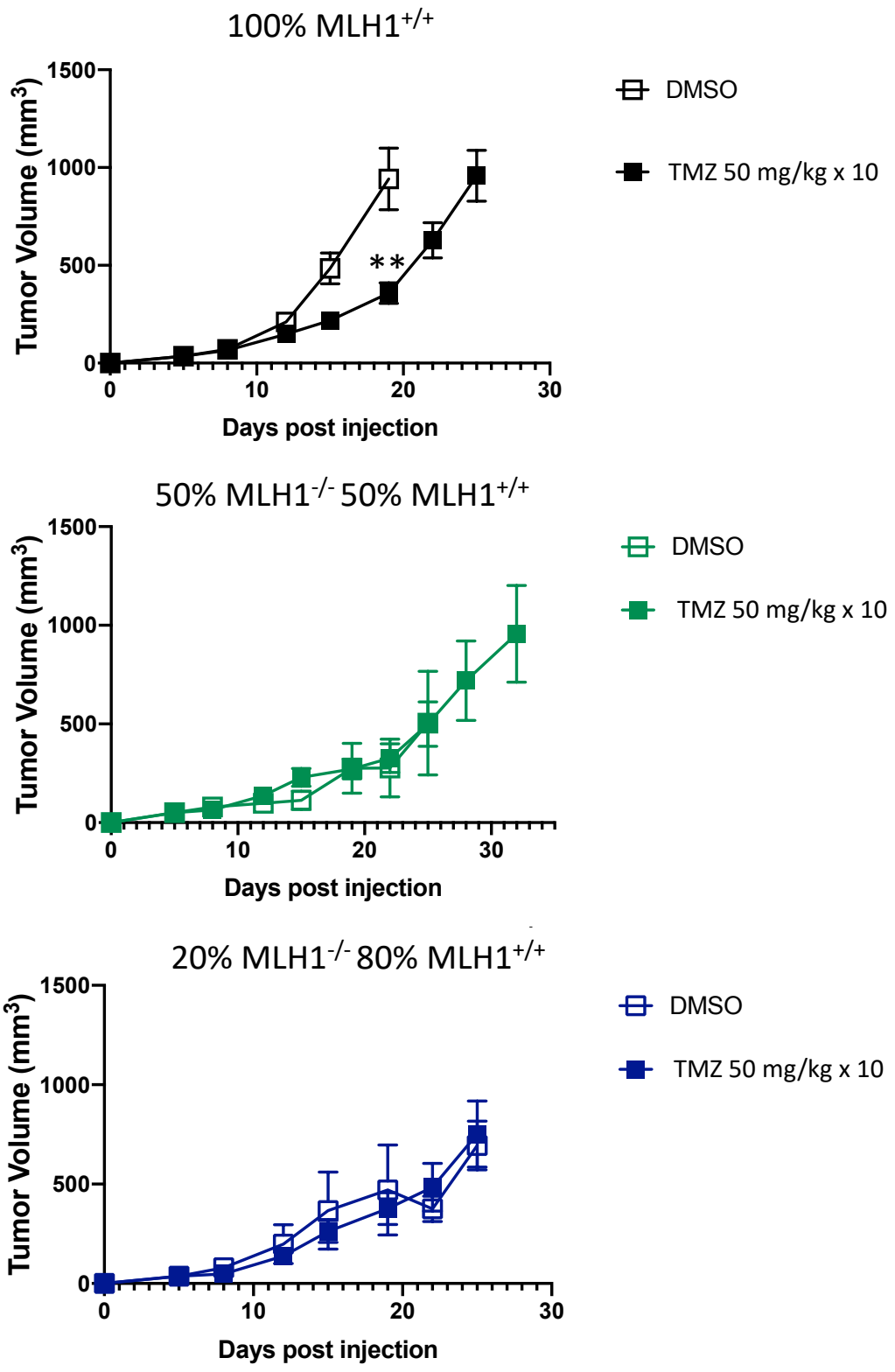
100% MLH1+/+
Tumor Volume (mm3)
1500
1000
500
0
0
10
20
30
Days post injection
**
DMSO
TMZ 50 mg/kg x 10
50% MLH1-/- 50% MLH1+/+
Tumor Volume (mm3)
1500
1000
500
0
0
10
20
30
Days post injection
DMSO
TMZ 50 mg/kg x 10
20% MLH1-/- 80% MLH1+/+
Tumor Volume (mm3)
1500
1000
500
0
0
10
20
30
Days post injection
DMSO
TMZ 50 mg/kg x 10

C

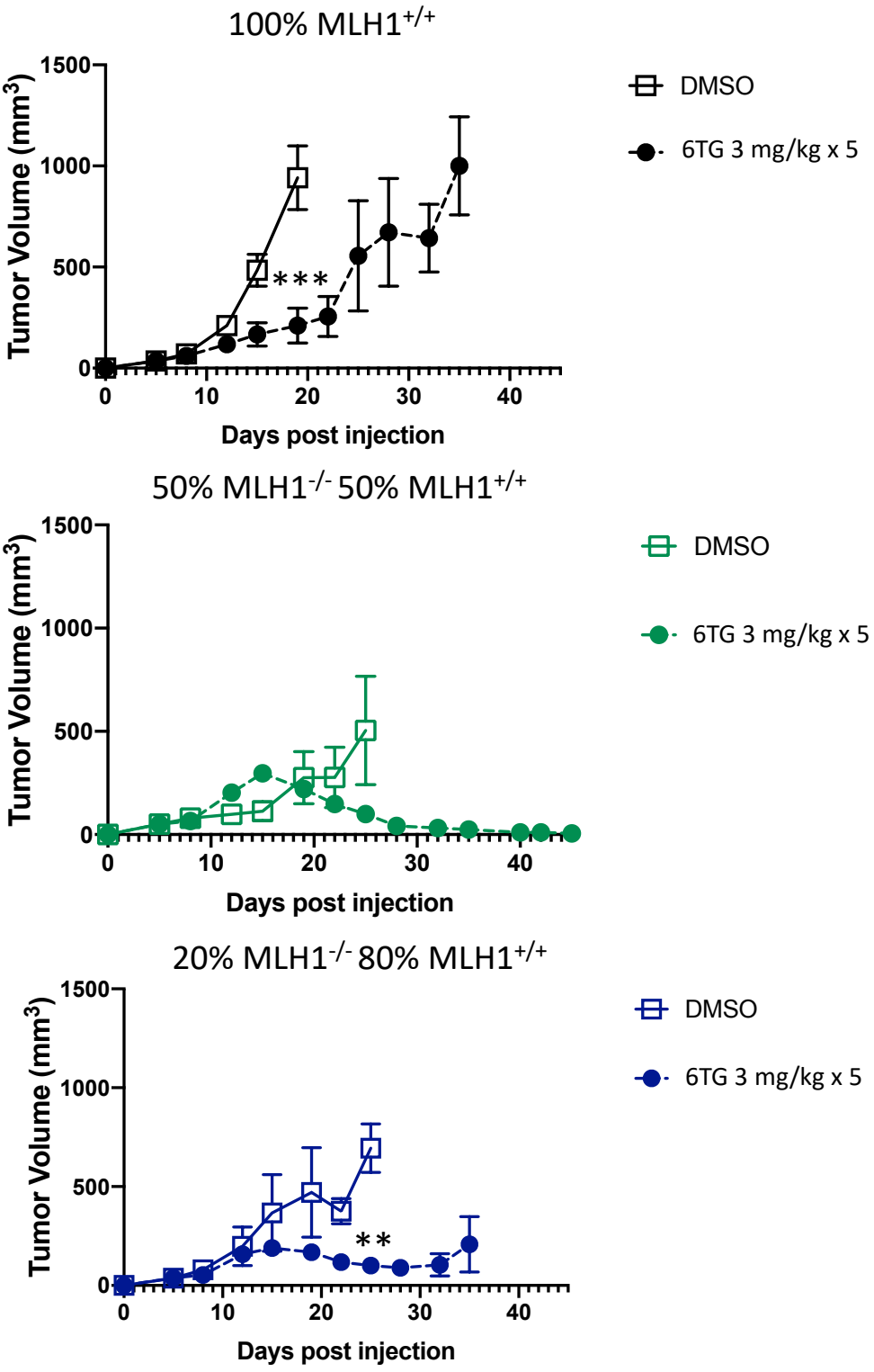
100% MLH1+/+
Tumor Volume (mm3)
1500
1000
500
0
0
10
20
30
40
Days post injection
***
DMSO
6TG 3 mg/kg x 5
50% MLH1-/- 50% MLH1+/+
Tumor Volume (mm3)
1500
1000
500
0
0
10
20
30
40
Days post injection
DMSO
6TG 3 mg/kg x 5
20% MLH1-/- 80% MLH1+/+
Tumor Volume (mm3)
1500
1000
500
0
0
10
20
30
40
Days post injection
**
DMSO
6TG 3 mg/kg x 5

Figure 20. In vivo treatment with 6-thioguanine delays growth of MMR heterogeneous tumor. A) *Graphical summary: CT26 MLH1 mixed populations (100% MLH1$^{+/+}$, 20% MLH1$^{-/-}$ 80% MLH1$^{+/+}$, 50% MLH1$^{-/-}$ 50% MLH1$^{+/+}$, 100% MLH1$^{-/-}$) were injected in immunocompetent mice (5 x 10^5 per mouse). 5 days post injection, mice were treated with* ***B)*** *TMZ 50 mg/kg (for 2 weeks, 5 days per week) or* ***C)*** *6TG 3mg/kg (for 5 days). DMSO treated mice served as controls. Mice tumor volume was measured twice a week and reported in the graph as average ± SEM. Each experimental group was composed at least of 10 animals. Statistical significance was evaluated by Mann-Whitney test:* *p<0,05, **p<0,005, *** p<0,0005

TMZ treatment slightly impacted MMRp and MMR heterogeneous tumor growth (**Fig 20 B**). On the contrary 6TG was more effective and induced a more prominent tumor growth delay in 100% MLH1$^{+/+}$ population (**Fig 20 C, Fig 21 A**). Next, we assessed the in vivo efficacy of 6TG treatment on a CT26 50% MLH1$^{-/-}$ 50% MLH1$^{+/+}$. As expected, the untreated control mice presented a heterogeneous response, with some tumors outgrowing and others being rejected. On the contrary, the 6TG treated arm showed a tumor growth impairment (**Fig 20 C**). Indeed, after an initial progression, all 6TG treated tumors started to shrink leading to complete tumor regression in all but three animals (**Fig 21 B**). Three out of ten mice presented a small mass that remained stable over time, while the remaining animals were tumor free until the end of the experiment (**Fig 21 B**). Fascinated by these results, we repeated the experiment starting from a population that was 20% MLH1$^{-/-}$ 80% MLH1$^{+/+}$. Also in this setting, in which the starting MMRd component was unfavoured, 6TG treatment induced major tumor regressions in 8 out of 10 animals (**Fig 20 C, Fig 21 C**).

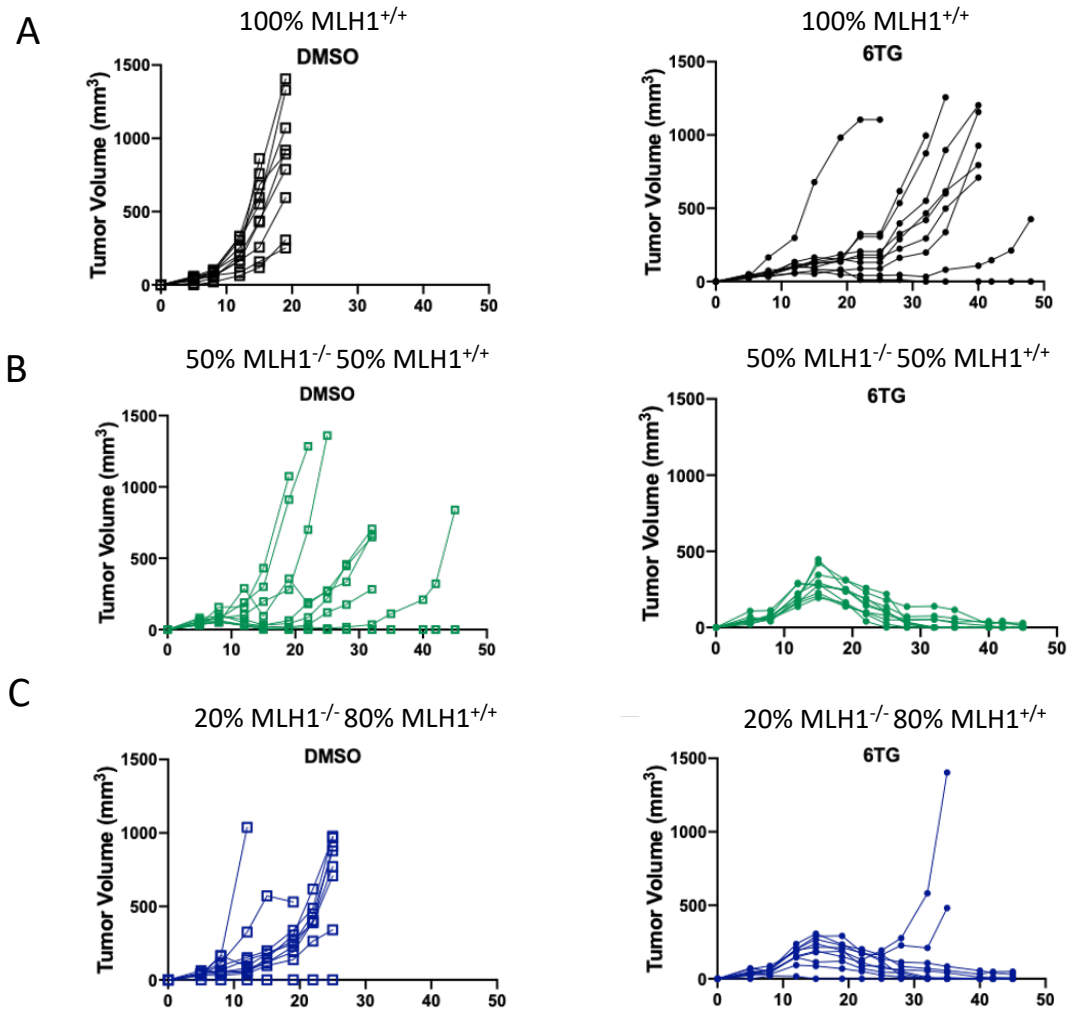

Figure 21. 6-thioguanine in vivo treatment leads to rejection of MMR heterogeneous tumor. *In this figure, single mice graphs of experiment in figure 20 are reported. In particular, CT26 100% MLH1$^{+/+}$(**A**), 50% MLH1$^{-/-}$ 50% MLH1$^{+/+}$ (**B**) and 20% MLH1$^{-/-}$ 80% MLH1$^{+/+}$ (**C**) cell populations were injected in immunocompetent mice (5 x 10^5 per mouse). 5 days post injection, mice were treated with 6TG 3mg/kg or DMSO as indicated in the legend of fig 20. Mice tumor volume was measured twice a week and reported in the graph as single mice values (mm^3). Each experimental group was composed at least of 10 animals.*

Additionally, responses were long lasting and mice remained tumor free until 120 days, after which they were sacrificed. These data demonstrate that genetical and pharmacological modulation cooperate in fostering immune surveillance of MMR heterogeneous tumor.

6. DISCUSSION

In this work we investigated whether and to what extent the presence of a MMRd fraction in MMR proficient tumors establishes cancer immune surveillance. We found that MMR heterogeneity has a profound effect on immune response in murine colorectal cancer models. We also demonstrated that the pharmacological selection of MMRd cells triggers enhanced cancer immune surveillance and limits immune evasion in MMR heterogeneous tumors.

Patients with tumors exhibiting microsatellite instability MSI/MMRd are characterized by a vigorous immune environment that predisposes for immune-based therapies success [16, 25, 39, 65, 66]. Oppositely, MSS/MMRp tumors are immunologically "cold" and refractory to immune-stimulating approaches. However, a subset of colorectal cancers is MMR heterogeneous, containing variable fractions of MMRp and MMRd cells in the same tumor [87, 92]. Heterogeneous patterns of MMR protein staining, as assessed by IHC, mirrors heterogeneity observed at the molecular level. Indeed, micro dissected areas displaying clonal loss of MMR proteins were associated with MSI status and MMR gene alterations [85, 90]. It is therefore tempting to speculate that this molecular feature impacts immune surveillance, immune evasion and response to immune therapies in CRC.

Few and contrasting observations arise from the clinic. Loupakis and colleagues associated the coexistence of MMRp and MMRd component in the same lesion of a CRC patient to a prolonged disease stabilization under immunotherapy treatment; these data suggest that a MSI component predisposes tumor to immune surveillance [92]. Oppositely, data from Kim and colleagues support an alternative hypothesis which identifies a correlation between MMR heterogeneity and pembrolizumab resistance in a metastatic gastric patient [88].

Taking advantage of syngeneic models harbouring proficient or deficient MMR machinery (generated in the hosting laboratory), we studied the effects of MMR heterogeneity on immune system activation and immune surveillance through the

injection of CT26 colorectal cancer cell populations in mice. We generated a spectrum of MMR heterogeneous tumor populations by mixing $MLH1^{+/+}$ and $MLH1^{-/-}$ cells at varying ratios in order to resemble different possible clinical scenarios. We demonstrated that the coexistence of MSS and MSI cells profoundly affects immune surveillance in murine CRC model. The effectiveness of the immune response is proportional to the fraction of MMRd cells present in the tumor mass. Notably, a fraction of the tumors in which MMRd cells constituted the majority of the cancer cell population were completely rejected by immunocompetent mice. These data suggest that MMRd cells could prime the immune system also against the proficient counterpart. Accordingly, this effect was immune driven and indeed was completely lost if the experiment was conducted in NODSCID mice, in which the immune system was severely compromised.

To date, conversion of immunologically "cold" into "hot" tumors is one of the most urgent clinical needs, as it could potentially increase the fraction of CRC patients eligible for immune-based therapy. In this context, the observation that a MMRp tumor harbouring a small fraction of MMRd cells can elicit an effective immune reaction, is highly promising. We demonstrated that the MSI component, even when minor, was pivotal in inducing a hot immune environment, by generating an increase of cytotoxic T cell infiltration. Accordingly, MMR heterogenous tumor rejection is observed only when the MMRd and MMRp fraction coexist in the same shared microenvironment, suggesting a pivotal role of local infiltration.

Although the immune response against MMR mixed tumors was remarkable compared to MSS tumors, the phenotype observed was heterogeneous, with some mice that were completely cured and others that experienced disease progression. We aimed at understanding the mechanism underlying the outgrowth of the MMR heterogeneous tumor by characterizing the MSS and MSI composition. We optimized a ddPCR assay, extremely specific and sensitive for the detection of $MLH1^{+/+}$ or $MLH1^{-/-}$ cells. The genetic analyses of escaped tumors revealed that the MMRp component drives immune escape, limiting immune surveillance and regenerating prevalently MSS tumor. Indeed, in all cases, the amount of $MLH1^{+/+}$

cells was increased compared to the day of injection. Moreover, the MSS component was dominant after immune editing and immune evasion also in tumors initially harbouring a small fraction of $MLH1^{+/+}$ cells. These data revealed that, as expected, in some cases MSS cells are able to do immune evasion; the percentage of MMRd cells is not enough to generate an effective response against the MMRp component, and immune editing remains limited to the MSI tumor. Moreover, risk of tumor outgrow increases with the percentage of MMRp cells in the mixed population. Intrigued by these results, we reasoned on the possibility to pharmacologically enhance the immune surveillance, by enriching the MMRd component in an MMR heterogeneous tumors. With this aim, we tested two anticancer agents, TMZ and 6TG, to select and enrich MMRd cells. We demonstrated that in vitro treatments of mixed population (MMRp and MMRd) with 6TG and TMZ rapidly increased MMRd fraction; in addition, cells that were treated with 6TG and TMZ in vitro were then injected in immune competent mice triggering a prolific immune response compared to unselected population.

Finally, we investigated whether in vivo treatments with TMZ and 6TG potentiate immune surveillance of MMR heterogeneous tumors. In colorectal cancer murine model, TMZ treatment had no impact in terms of tumor immune control. On the contrary, in vivo 6TG treatment of MMR heterogeneous tumors greatly fostered cancer immune surveillance and significantly limited immune evasion, hindering MMRp subclonal component outgrowth. Indeed, upon 6TG treatment, the majority of mice harbouring MMR heterogeneous tumor were cured while MSS tumor experienced only a partial tumor growth delay. We speculated that 6TG treatment of MMR heterogeneous tumors reduces MSS component, determining the enrichment of the MSI counterpart. An increased percentage of MMRd cells results in a stronger activation of the immune system, leading to complete MMR heterogeneous tumor elimination. Oppositely, despite in vitro experiment remarkable results, in vivo TMZ treatment failed in promoting immune response in MMR heterogeneous murine tumors. As many chemotherapeutic agents, one of the main adverse events related to TMZ therapy is immune suppression [105, 106]. We speculated that the prolonged and high dose TMZ treatment in vivo led

to immune suppression, thus impairing immune activation induced by MMRd cells.

Despite extensive efforts in generating a murine model of MMR heterogeneity, this fails in recapitulating the complexity of the human disease. In details, murine MMR heterogeneous tumors have been generated mixing two different clones (MLH1 $^{+/+}$ and MLH1 $^{-/-}$) with specific genetic background and phenotypical properties; this strategy results in a model which is still far from the human condition, in which the dynamics of the generation of MMR heterogeneous tumor are more complex and thus still completely unknow. In addition, a murine model composed by two clones artificially reduces human disease heterogeneity, in which several subpopulations coexist. Moreover, the exact composition of MMRp and MMRd in human MMR heterogeneous CRC is unknown. Accordingly, we chose a large spectrum of MSS/MSI cell ratios, aimed to investigate different possible MMR heterogeneous tumor scenarios.

We also proposed a simple characterization of MMR heterogenous tumor immune infiltration based on CD4+ and CD8+ T cells, without providing functional evidences regarding their role in MMR heterogeneous tumor immune surveillance. Anyway, although human tumor immune infiltrate is highly complex and dynamic, as it includes innate and adaptive immune players, stromal cells and soluble factors, our evidences suggest that a punctual analyses of the immune infiltrate in human MMR heterogeneous tumors could reveal unknown patterns, possibly exploitable to design strategy aimed to increase immune response.

Our work also suggests that drugs which selects for MMR deficient cells might in principle be used to increase immune surveillance of MSS CRC patients. In this regard, 6-Thioguanine and Temozolomide are not commonly used in CRC given the low anti-tumor activity observed so far in clinical trial. However, several reports highlighted that MMR deficiency is one of the key mechanisms of resistance that emerge under 6TG or TMZ treatment in clinical practice [98, 104, 107]. MMR heterogeneous tumour treatment with chemicals such as 6TG or TMZ, despite the limited clinical impact measured by RECIST criteria, might

alter the tumor genetic background, favouring the emergence of the MMRd component. This in turn could increase the possibility of response to checkpoint inhibitors in CRC. In this regard, a recently completed clinical trial (MAYA, NCT03832621) explored the combination of temozolomide with nivolumab and ipilimumab to treat MSS metastatic CRC patients. The initial MAYA results are encouraging with a 42% reported response rate [108].

Notwithstanding the limits of the artefactual MMR model generated in our work, we propose a proof-of-concept study in which we highlight the relevance of a correct MMR status definition in CRC, with possible implications in terms of immune surveillance and immune evasion. Additionally, we support our idea regarding the use of FDA approved compounds to enrich MMRd cells improving outcome of MMR heterogeneous tumors.

7. CONCLUSIONS AND FUTURE PERSPECTIVES

MMR status is currently a fundamental biomarker that drives therapeutic design and profoundly affects CRC patient prognosis. In this work, we highlighted the importance of the MMR heterogeneity, a condition neglected in the past that hides potential important clinical implications for a group of CRC patients. Indeed, we demonstrated that a fraction of MMRd cells in a MMRp tumors, affects immune surveillance and perturbates the immune infiltrate, predisposing to immune response. We also demonstrated that MMR heterogeneity could be modulated by exploiting FDA approved agents, that can cooperate to generate a hot and responsive immune environment. Our data suggest that MMR heterogeneity is an important condition that should be taken into account during pathological analyses. Indeed, a more extensive and deep characterization of biopsy fragments could reveal a major number of MMR heterogeneous cases increasing the number of MMR heterogeneous patients. Patients carrying MMR heterogeneous tumors could be candidates for immune based approach, increasing the number of CRC patients that could benefit from CPIs, an actual urgent clinical need.

As future perspectives, further studies are needed to consolidate our findings. We will expand murine models tested to understand if the phenotype observed is tissue specific or has relevance in several settings. We will expand the immune characterization performed, including other innate and adaptive immune players, evaluating their infiltration and markers of activations. We will also investigate the immunological mechanisms at the base of MMR heterogeneous tumor immune surveillance. As reported in the introduction, several mechanisms are involved in MMRd tumors response, including cGAS-STING pathway activation and neoantigen dependent response. To reach our goal, we will perform the "mixing experiment" exploiting Beta 2 microglobulin knock out cell lines (with compromised antigen presentation) [109], but also recently generated cGAS wild type and knockout models (**Fig 22**) .

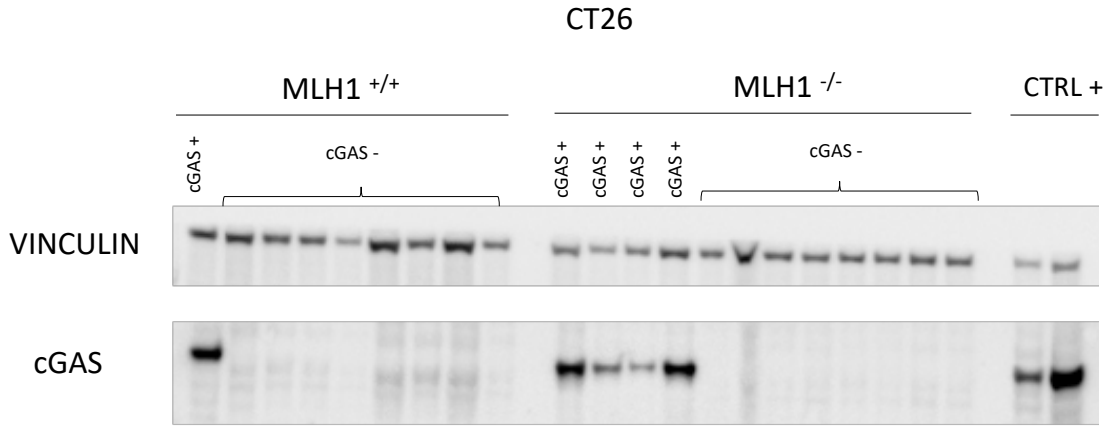

Figure 22. cGAS expression in CT26 clones. *cGAS protein was inactivated in CT26 MLH1$^{+/+}$ and MLH1$^{-/-}$ clones using CRISPR Cas9 technology. In the figure, Western Blot of cGAS wt (+) and cGAS* ko (-) *clones is reported. Actin and Vinculin served as loading control*

Preliminary experiments confirmed that impairment of cGAS pathway limits immune surveillance of MMRd tumors. Indeed, while MLH1$^{-/-}$ cGAS$^{+/+}$ clone was not able to generate tumors when injected in immunocompetent environment, clones lacking cGAS expression presented a heterogeneous phenotype, with mice completely cured and mice growing overtime (3/6 clone 5, 2/6 clone 1) (**Fig 23**)

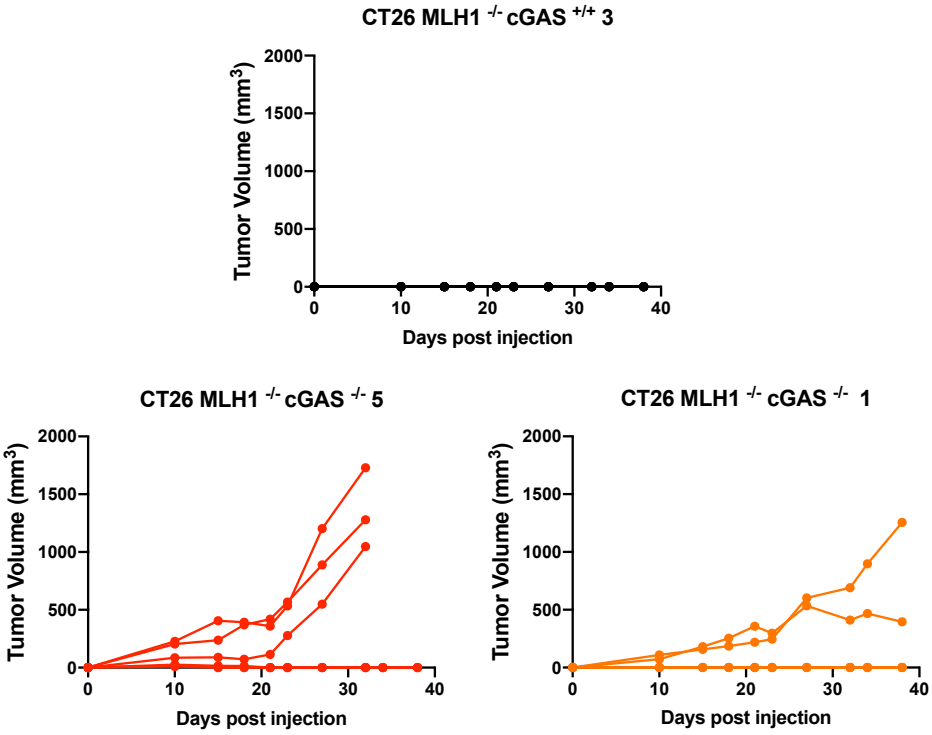

Figure 23. cGAS knock out partially impairs the immune surveillance of MMRd cells*. CT26 MLH1$^{-/-}$ cGAS$^{-/-}$ or cGAS$^{+/+}$ cells were subcutaneously injected in immunocompetent mice (5 x 10^5 cells per mice). Tumor growth was monitored overtime. At least 5 mice for each clone were injected. Graphs represent the tumor growth of single mice.*

In summary, this is a proof-of-concept study that underlies the importance of a correct MMR status definition and that demonstrates the impact of MMR heterogeneity on murine CRC immune surveillance. Finally, our data suggest that MMR heterogeneity is an exploitable feature to modulate tumor immune environment predisposing to the success of immune response.

REFERENCES

1. Siegel, R.L., K.D. Miller, and A. Jemal, *Cancer statistics, 2020.* CA Cancer J Clin, 2020. **70**(1): p. 7-30.
2. Amodio, V., et al., *Mechanisms of Immune Escape and Resistance to Checkpoint Inhibitor Therapies in Mismatch Repair Deficient Metastatic Colorectal Cancers.* Cancers (Basel), 2021. **13**(11).
3. Van Cutsem, E., et al., *ESMO consensus guidelines for the management of patients with metastatic colorectal cancer.* Ann Oncol, 2016. **27**(8): p. 1386-422.
4. DeSantis, C.E., et al., *Cancer treatment and survivorship statistics, 2014.* CA Cancer J Clin, 2014. **64**(4): p. 252-71.
5. Jiricny, J., *The multifaceted mismatch-repair system.* Nat Rev Mol Cell Biol, 2006. **7**(5): p. 335-46.
6. Gupta, R., S. Sinha, and R.N. Paul, *The impact of microsatellite stability status in colorectal cancer.* Curr Probl Cancer, 2018. **42**(6): p. 548-559.
7. Ganesh, K., et al., *Immunotherapy in colorectal cancer: rationale, challenges and potential.* Nat Rev Gastroenterol Hepatol, 2019. **16**(6): p. 361-375.
8. Koopman, M., et al., *Deficient mismatch repair system in patients with sporadic advanced colorectal cancer.* Br J Cancer, 2009. **100**(2): p. 266-73.
9. Sinicrope, F.A. and D.J. Sargent, *Molecular pathways: microsatellite instability in colorectal cancer: prognostic, predictive, and therapeutic implications.* Clin Cancer Res, 2012. **18**(6): p. 1506-12.
10. Herman, J.G., et al., *Incidence and functional consequences of hMLH1 promoter hypermethylation in colorectal carcinoma.* Proc Natl Acad Sci U S A, 1998. **95**(12): p. 6870-5.
11. Venderbosch, S., et al., *Mismatch repair status and BRAF mutation status in metastatic colorectal cancer patients: a pooled analysis of the CAIRO,*

CAIRO2, COIN, and FOCUS studies. Clin Cancer Res, 2014. **20**(20): p. 5322-30.

12. De Smedt, L., et al., *Microsatellite instable vs stable colon carcinomas: analysis of tumour heterogeneity, inflammation and angiogenesis.* Br J Cancer, 2015. **113**(3): p. 500-9.
13. Benatti, P., et al., *Microsatellite instability and colorectal cancer prognosis.* Clin Cancer Res, 2005. **11**(23): p. 8332-40.
14. Tougeron, D., et al., *Prognosis and chemosensitivity of deficient MMR phenotype in patients with metastatic colorectal cancer: An AGEO retrospective multicenter study.* Int J Cancer, 2020. **147**(1): p. 285-296.
15. Le, D.T., et al., *PD-1 Blockade in Tumors with Mismatch-Repair Deficiency.* N Engl J Med, 2015. **372**(26): p. 2509-20.
16. Overman, M.J., et al., *Durable Clinical Benefit With Nivolumab Plus Ipilimumab in DNA Mismatch Repair-Deficient/Microsatellite Instability-High Metastatic Colorectal Cancer.* J Clin Oncol, 2018. **36**(8): p. 773-779.
17. Rousseau, B., et al., *The Spectrum of Benefit from Checkpoint Blockade in Hypermutated Tumors.* N Engl J Med, 2021. **384**(12): p. 1168-1170.
18. Turajlic, S., et al., *Insertion-and-deletion-derived tumour-specific neoantigens and the immunogenic phenotype: a pan-cancer analysis.* Lancet Oncol, 2017. **18**(8): p. 1009-1021.
19. Boland, C.R. and A. Goel, *Microsatellite instability in colorectal cancer.* Gastroenterology, 2010. **138**(6): p. 2073-2087.e3.
20. Ciardiello, D., et al., *Immunotherapy of colorectal cancer: Challenges for therapeutic efficacy.* Cancer Treat Rev, 2019. **76**: p. 22-32.
21. Durno, C.A., et al., *Phenotypic and genotypic characterisation of biallelic mismatch repair deficiency (BMMR-D) syndrome.* Eur J Cancer, 2015. **51**(8): p. 977-83.
22. Alexandrov, L.B., et al., *The repertoire of mutational signatures in human cancer.* Nature, 2020. **578**(7793): p. 94-101.

23. Haradhvala, N.J., et al., *Distinct mutational signatures characterize concurrent loss of polymerase proofreading and mismatch repair.* Nat Commun, 2018. **9**(1): p. 1746.
24. Chung, J., et al., *DNA polymerase and mismatch repair exert distinct microsatellite instability signatures in normal and malignant human cells.* Cancer Discov, 2020.
25. Benson, A.B., et al., *Colon Cancer, Version 2.2021, NCCN Clinical Practice Guidelines in Oncology.* J Natl Compr Canc Netw, 2021. **19**(3): p. 329-359.
26. Yoshino, T., et al., *Pan-Asian adapted ESMO consensus guidelines for the management of patients with metastatic colorectal cancer: a JSMO-ESMO initiative endorsed by CSCO, KACO, MOS, SSO and TOS.* Ann Oncol, 2018. **29**(1): p. 44-70.
27. Becht, E., et al., *Immune and Stromal Classification of Colorectal Cancer Is Associated with Molecular Subtypes and Relevant for Precision Immunotherapy.* Clin Cancer Res, 2016. **22**(16): p. 4057-66.
28. Picard, E., et al., *Relationships Between Immune Landscapes, Genetic Subtypes and Responses to Immunotherapy in Colorectal Cancer.* Front Immunol, 2020. **11**: p. 369.
29. Galon, J., et al., *Type, density, and location of immune cells within human colorectal tumors predict clinical outcome.* Science, 2006. **313**(5795): p. 1960-4.
30. Galon, J., et al., *Towards the introduction of the 'Immunoscore' in the classification of malignant tumours.* J Pathol, 2014. **232**(2): p. 199-209.
31. Argilés, G., et al., *Localised colon cancer: ESMO Clinical Practice Guidelines for diagnosis, treatment and follow-up.* Ann Oncol, 2020. **31**(10): p. 1291-1305.
32. Pagès, F., et al., *International validation of the consensus Immunoscore for the classification of colon cancer: a prognostic and accuracy study.* Lancet, 2018. **391**(10135): p. 2128-2139.

33. Huyghe, N., P. Baldin, and M. Van den Eynde, *Immunotherapy with immune checkpoint inhibitors in colorectal cancer: what is the future beyond deficient mismatch-repair tumours?* Gastroenterol Rep (Oxf), 2020. **8**(1): p. 11-24.

34. Al-Shibli, K.I., et al., *Prognostic effect of epithelial and stromal lymphocyte infiltration in non-small cell lung cancer.* Clin Cancer Res, 2008. **14**(16): p. 5220-7.

35. Hiraoka, K., et al., *Concurrent infiltration by CD8+ T cells and CD4+ T cells is a favourable prognostic factor in non-small-cell lung carcinoma.* Br J Cancer, 2006. **94**(2): p. 275-80.

36. Maby, P., et al., *Correlation between Density of CD8+ T-cell Infiltrate in Microsatellite Unstable Colorectal Cancers and Frameshift Mutations: A Rationale for Personalized Immunotherapy.* Cancer Res, 2015. **75**(17): p. 3446-55.

37. Kim, H., et al., *Clinical and pathological characteristics of sporadic colorectal carcinomas with DNA replication errors in microsatellite sequences.* Am J Pathol, 1994. **145**(1): p. 148-56.

38. Guidoboni, M., et al., *Microsatellite instability and high content of activated cytotoxic lymphocytes identify colon cancer patients with a favorable prognosis.* Am J Pathol, 2001. **159**(1): p. 297-304.

39. Llosa, N.J., et al., *The vigorous immune microenvironment of microsatellite instable colon cancer is balanced by multiple counter-inhibitory checkpoints.* Cancer Discov., 2015. **5**(1): p. 43–51.

40. Lin, A., J. Zhang, and P. Luo, *Crosstalk Between the MSI Status and Tumor Microenvironment in Colorectal Cancer.* Front Immunol, 2020. **11**: p. 2039.

41. Angell, H.K., et al., *The Immunoscore: Colon Cancer and Beyond.* Clin Cancer Res, 2020. **26**(2): p. 332-339.

42. Gulubova, M.V., et al., *Role of dendritic cells in progression and clinical outcome of colon cancer.* Int J Colorectal Dis, 2012. **27**(2): p. 159-69.
43. Dadabayev, A.R., et al., *Dendritic cells in colorectal cancer correlate with other tumor-infiltrating immune cells.* Cancer Immunol Immunother, 2004. **53**(11): p. 978-86.
44. Bauer, K., et al., *Dendritic cell and macrophage infiltration in microsatellite-unstable and microsatellite-stable colorectal cancer.* Fam Cancer, 2011. **10**(3): p. 557-65.
45. Germano, G., et al., *The Clinical Impact of the Genomic Landscape of Mismatch Repair-Deficient Cancers.* Cancer Discov, 2018. **8**(12): p. 1518-1528.
46. Rospo, G., et al., *Evolving neoantigen profiles in colorectal cancers with DNA repair defects.* Genome Med, 2019. **11**(1): p. 42.
47. Kosugi, S., et al., *Comprehensive evaluation of structural variation detection algorithms for whole genome sequencing.* Genome Biol, 2019. **20**(1): p. 117.
48. Germano, G., et al., *Inactivation of DNA repair triggers neoantigen generation and impairs tumour growth.* Nature, 2017. **552**(7683): p. 116-120.
49. Nakayama, M., *Antigen Presentation by MHC-Dressed Cells.* Front Immunol, 2014. **5**: p. 672.
50. Mardis, E.R., *Neoantigens and genome instability: impact on immunogenomic phenotypes and immunotherapy response.* Genome Med, 2019. **11**(1): p. 71.
51. Bjerregaard, A.M., et al., *MuPeXI: prediction of neo-epitopes from tumor sequencing data.* Cancer Immunol Immunother, 2017. **66**(9): p. 1123-1130.
52. Richters, M.M., et al., *Best practices for bioinformatic characterization of neoantigens for clinical utility.* Genome Med, 2019. **11**(1): p. 56.

53. Hundal, J., et al., *pVAC-Seq: A genome-guided in silico approach to identifying tumor neoantigens.* Genome Med, 2016. **8**(1): p. 11.
54. Segal, N.H., et al., *Epitope landscape in breast and colorectal cancer.* Cancer Res, 2008. **68**(3): p. 889-92.
55. Gubin, M.M., et al., *Checkpoint blockade cancer immunotherapy targets tumour-specific mutant antigens.* Nature, 2014. **515**(7528): p. 577-81.
56. Giannakis, M., et al., *Genomic Correlates of Immune-Cell Infiltrates in Colorectal Carcinoma.* Cell Rep, 2016. **15**(4): p. 857-865.
57. Gubin, M.M. and R.D. Schreiber, *CANCER. The odds of immunotherapy success.* Science, 2015. **350**(6257): p. 158-9.
58. Van Allen, E.M., et al., *Genomic correlates of response to CTLA-4 blockade in metastatic melanoma.* Science, 2015. **350**(6257): p. 207-211.
59. Leoni, G., et al., *A Genetic Vaccine Encoding Shared Cancer Neoantigens to Treat Tumors with Microsatellite Instability.* Cancer Res, 2020. **80**(18): p. 3972-3982.
60. Roudko, V., et al., *Shared Immunogenic Poly-Epitope Frameshift Mutations in Microsatellite Unstable Tumors.* Cell, 2020. **183**(6): p. 1634-1649.e17.
61. Ballhausen, A., et al., *The shared frameshift mutation landscape of microsatellite-unstable cancers suggests immunoediting during tumor evolution.* Nat Commun, 2020. **11**(1): p. 4740.
62. Laumont, C.M., et al., *Global proteogenomic analysis of human MHC class I-associated peptides derived from non-canonical reading frames.* Nat Commun, 2016. **7**: p. 10238.
63. Darvin, P., et al., *Immune checkpoint inhibitors: recent progress and potential biomarkers.* Exp Mol Med, 2018. **50**(12): p. 1-11.
64. André, T., et al., *Pembrolizumab in Microsatellite-Instability-High Advanced Colorectal Cancer.* N Engl J Med, 2020. **383**(23): p. 2207-2218.
65. Lenz, H.-J., et al., *Nivolumab (NIVO) + low-dose ipilimumab (IPI) as first-line (1L) therapy in microsatellite instability-high/DNA mismatch repair*

deficient (MSI-H/dMMR) metastatic colorectal cancer (mCRC): Clinical update. 2019: Journal of Clinical Oncology.

66. Lenz, H.-J., et al., *Subgroup analyses of patients (pts) with microsatellite instability-high/mismatch repair-deficient (MSI-H/dMMR) metastatic colorectal cancer (mCRC) treated with nivolumab (NIVO) plus low-dose ipilimumab (IPI) as first-line (1L) therapy:Two-year clinical update.* Journal of Clinical Oncology, 2021. **39**(3_suppl): p. 58-58.
67. Cohen, R., et al., *Immune Checkpoint Inhibition in Metastatic Colorectal Cancer Harboring Microsatellite Instability or Mismatch Repair Deficiency.* Cancers (Basel), 2021. **13**(5).
68. Chalabi, M., et al., *Neoadjuvant immunotherapy leads to pathological responses in MMR-proficient and MMR-deficient early-stage colon cancers.* Nat Med, 2020. **26**(4): p. 566-576.
69. Lu, C., et al., *DNA Sensing in Mismatch Repair-Deficient Tumor Cells Is Essential for Anti-tumor Immunity.* Cancer Cell, 2021. **39**(1): p. 96-108.e6.
70. Decout, A., et al., *The cGAS-STING pathway as a therapeutic target in inflammatory diseases.* Nat Rev Immunol, 2021. **21**(9): p. 548-569.
71. He, L., et al., *Nucleic acid sensing pattern recognition receptors in the development of colorectal cancer and colitis.* Cell Mol Life Sci, 2017. **74**(13): p. 2395-2411.
72. Ho, S.S., et al., *The DNA Structure-Specific Endonuclease MUS81 Mediates DNA Sensor STING-Dependent Host Rejection of Prostate Cancer Cells.* Immunity, 2016. **44**(5): p. 1177-89.
73. Lemos, H., et al., *STING Promotes the Growth of Tumors Characterized by Low Antigenicity via IDO Activation.* Cancer Res, 2016. **76**(8): p. 2076-81.
74. Chen, Q., et al., *Carcinoma-astrocyte gap junctions promote brain metastasis by cGAMP transfer.* Nature, 2016. **533**(7604): p. 493-498.
75. Du, H., T. Xu, and M. Cui, *cGAS-STING signaling in cancer immunity and immunotherapy.* Biomed Pharmacother, 2021. **133**: p. 110972.

76. Gerlinger, M., *Immunotherapy Sensitivity of Mismatch Repair-Deficient Cancer: Mutation Load Is Not Enough.* Cancer Cell, 2021. **39**(1): p. 16-18.
77. Wang, Z., et al., *cGAS/STING axis mediates a topoisomerase II inhibitor-induced tumor immunogenicity.* J Clin Invest, 2019. **129**(11): p. 4850-4862.
78. Marcus, A., et al., *Tumor-Derived cGAMP Triggers a STING-Mediated Interferon Response in Non-tumor Cells to Activate the NK Cell Response.* Immunity, 2018. **49**(4): p. 754-763.e4.
79. Schadt, L., et al., *Cancer-Cell-Intrinsic cGAS Expression Mediates Tumor Immunogenicity.* Cell Rep, 2019. **29**(5): p. 1236-1248.e7.
80. Woo, S.R., et al., *STING-dependent cytosolic DNA sensing mediates innate immune recognition of immunogenic tumors.* Immunity, 2014. **41**(5): p. 830-42.
81. Lam, A.R., et al., *RAE1 ligands for the NKG2D receptor are regulated by STING-dependent DNA sensor pathways in lymphoma.* Cancer Res, 2014. **74**(8): p. 2193-2203.
82. Takashima, K., et al., *STING in tumor and host cells cooperatively work for NK cell-mediated tumor growth retardation.* Biochem Biophys Res Commun, 2016. **478**(4): p. 1764-71.
83. Guan, J., et al., *MLH1 Deficiency-Triggered DNA Hyperexcision by Exonuclease 1 Activates the cGAS-STING Pathway.* Cancer Cell, 2021. **39**(1): p. 109-121.e5.
84. Ng, K.W., et al., *cGAS-STING and Cancer: Dichotomous Roles in Tumor Immunity and Development.* Trends Immunol, 2018. **39**(1): p. 44-54.
85. McCarthy, A.J., et al., *Heterogenous loss of mismatch repair (MMR) protein expression: a challenge for immunohistochemical interpretation and microsatellite instability (MSI) evaluation.* J Pathol Clin Res, 2019. **5**(2): p. 115-129.

86. Fusco, N., et al., *Mismatch Repair Protein Loss as a Prognostic and Predictive Biomarker in Breast Cancers Regardless of Microsatellite Instability.* JNCI Cancer Spectr, 2018. **2**(4): p. pky056.
87. Chapusot, C., et al., *Microsatellite instability and intratumoural heterogeneity in 100 right-sided sporadic colon carcinomas.* Br J Cancer, 2002. **87**(4): p. 400-4.
88. Kim, S.T., et al., *Comprehensive molecular characterization of clinical responses to PD-1 inhibition in metastatic gastric cancer.* Nat Med, 2018. **24**(9): p. 1449-1458.
89. Renkonen, E., et al., *Altered expression of MLH1, MSH2, and MSH6 in predisposition to hereditary nonpolyposis colorectal cancer.* J Clin Oncol, 2003. **21**(19): p. 3629-37.
90. Joost, P., et al., *Heterogenous mismatch-repair status in colorectal cancer.* Diagn Pathol, 2014. **9**: p. 126.
91. Watson, N., et al., *Heterogeneous staining for mismatch repair proteins during population-based prescreening for hereditary nonpolyposis colorectal cancer.* J Mol Diagn, 2007. **9**(4): p. 472-8.
92. Loupakis, F., et al., *Treatment with checkpoint inhibitors in a metastatic colorectal cancer patient with molecular and immunohistochemical heterogeneity in MSI/dMMR status.* J Immunother Cancer, 2019. **7**(1): p. 297.
93. Greenberg, A., et al., *Geographic Heterogeneity for Mismatch Repair Proteins Is Associated with Defects in DNA Repair.* Isr Med Assoc J, 2020. **22**(1): p. 32-36.
94. Watkins, J.C., et al., *Unusual Mismatch Repair Immunohistochemical Patterns in Endometrial Carcinoma.* Am J Surg Pathol, 2016. **40**(7): p. 909-16.

95. He, W.Z., et al., *Comparison of Mismatch Repair Status Between Primary and Matched Metastatic Sites in Patients With Colorectal Cancer.* J Natl Compr Canc Netw, 2019. **17**(10): p. 1174-1183.

96. Cohen, R., et al., *Association of Primary Resistance to Immune Checkpoint Inhibitors in Metastatic Colorectal Cancer With Misdiagnosis of Microsatellite Instability or Mismatch Repair Deficiency Status.* JAMA Oncol, 2019. **5**(4): p. 551-555.

97. Strobel, H., et al., *Temozolomide and Other Alkylating Agents in Glioblastoma Therapy.* Biomedicines, 2019. **7**(3).

98. Cahill, D.P., et al., *Loss of the mismatch repair protein MSH6 in human glioblastomas is associated with tumor progression during temozolomide treatment.* Clin Cancer Res, 2007. **13**(7): p. 2038-45.

99. Yip, S., et al., *MSH6 mutations arise in glioblastomas during temozolomide therapy and mediate temozolomide resistance.* Clin Cancer Res, 2009. **15**(14): p. 4622-9.

100. Yan, T., et al., *DNA mismatch repair (MMR) mediates 6-thioguanine genotoxicity by introducing single-strand breaks to signal a G2-M arrest in MMR-proficient RKO cells.* Clin Cancer Res, 2003. **9**(6): p. 2327-34.

101. Glaab, W.E., et al., *Resistance to 6-thioguanine in mismatch repair-deficient human cancer cell lines correlates with an increase in induced mutations at the HPRT locus.* Carcinogenesis, 1998. **19**(11): p. 1931-7.

102. Karran, P. and M. Bignami, *DNA damage tolerance, mismatch repair and genome instability.* Bioessays, 1994. **16**(11): p. 833-9.

103. Fink, D., S. Aebi, and S.B. Howell, *The role of DNA mismatch repair in drug resistance.* Clin Cancer Res, 1998. **4**(1): p. 1-6.

104. Evensen, N.A., et al., *MSH6 haploinsufficiency at relapse contributes to the development of thiopurine resistance in pediatric B-lymphoblastic leukemia.* Haematologica, 2018. **103**(5): p. 830-839.

105. Sengupta, S., et al., *Impact of temozolomide on immune response during malignant glioma chemotherapy.* Clin Dev Immunol, 2012. **2012**: p. 831090.

106. Wang, S., et al., *Temozolomide promotes immune escape of GBM cells via upregulating PD-L1.* Am J Cancer Res, 2019. **9**(6): p. 1161-1171.

107. Chen, L., et al., *Clinical efficacy and safety of 6-thioguanine in the treatment of childhood acute lymphoblastic leukemia: A protocol for systematic review and meta-analysis.* Medicine (Baltimore), 2020. **99**(18): p. e20082.

108. Pietrantonio F. , et al., *383O - MAYA trial: Temozolomide (TMZ) priming followed by combination with low-dose ipilimumab and nivolumab in patients with microsatellite stable (MSS), MGMT silenced metastatic colorectal cancer (mCRC)*. 2021: Annals of Oncology p. S530-S582.

109. Germano, G., et al., *CD4 T cell dependent rejection of beta 2 microglobulin null mismatch repair deficient tumors.* Cancer Discov, 2021.

VITO AMODIO

PhD Publications Report

Papers/Reviews

Mechanisms of Immune Escape and Resistance to Checkpoint Inhibitor Therapies in Mismatch Repair Deficient Metastatic Colorectal Cancers.

Amodio V, Mauri G, Reilly NM, Sartore-Bianchi A, Siena S, Bardelli A, Germano G.
Cancers (Basel). 2021 May 27;13(11):2638. doi: 10.3390/cancers13112638.
PMID: 34072037

CD4 T Cell-Dependent Rejection of Beta-2 Microglobulin Null Mismatch Repair-Deficient Tumors.

Germano G, Lu S, Rospo G, Lamba S, Rousseau B, Fanelli S, Stenech D, Le DT, Hays J, Totaro MG, Amodio V, Chilà R, Mondino A, Diaz LA Jr, Di Nicolantonio F, Bardelli A.
Cancer Discov. 2021 Mar 2. doi: 10.1158/2159-8290.CD-20-0987. Online ahead of print.
PMID: 33653693

T Cells Expressing Receptor Recombination/Revision Machinery Are Detected in the Tumor Microenvironment and Expanded in Genomically Over-unstable Models.

Morello G, Cancila V, La Rosa M, Germano G, Lecis D, Amodio V, Zanardi F, Iannelli F, Greco D, La Paglia L, Fiannaca A, Urso AM, Graziano G, Ferrari F, Pupa SM, Sangaletti S, Chiodoni C, Pruneri G, Bardelli A, Colombo MP, Tripodo C.
Cancer Immunol Res. 2021 May 3. doi: 10.1158/2326-6066.CIR-20-0645. Online ahead of print.
PMID: 33941587

EGFR Blockade Reverts Resistance to KRASG12C Inhibition in Colorectal Cancer.

Amodio V, Yaeger R, Arcella P, Cancelliere C, Lamba S, Lorenzato A, Arena S, Montone M, Mussolin B, Bian Y, Whaley A, Pinnelli M, Murciano-Goroff YR, Vakiani E, Valeri N, Liao WL, Bhalkikar A, Thyparambil S, Zhao HY, de Stanchina E, Marsoni S, Siena S, Bertotti A, Trusolino L, Li BT, Rosen N, Di Nicolantonio F, Bardelli A, Misale S.
Cancer Discov. 2020 Aug;10(8):1129-1139. doi: 10.1158/2159-8290.CD-20-0187. Epub 2020 May 19.
PMID: 32430388

High-dose vitamin C enhances cancer immunotherapy.

Magrì A, Germano G, Lorenzato A, Lamba S, Chilà R, Montone M, Amodio V, Ceruti T, Sassi F, Arena S, Abrignani S, D'Incalci M, Zucchetti M, Di Nicolantonio F, Bardelli A.
Sci Transl Med. 2020 Feb 26;12(532):eaay8707. doi: 10.1126/scitranslmed.aay8707.
PMID: 32102933

Adaptive mutability of colorectal cancers in response to targeted therapies.

Russo M, Crisafulli G, Sogari A, Reilly NM, Arena S, Lamba S, Bartolini A, Amodio V, Magrì A, Novara L, Sarotto I, Nagel ZD, Piett CG, Amatu A, Sartore-Bianchi A, Siena S, Bertotti A, Trusolino L, Corigliano M, Gherardi M, Lagomarsino MC, Di Nicolantonio F, Bardelli A.
Science. 2019 Dec 20;366(6472):1473-1480. doi: 10.1126/science.aav4474. Epub 2019 Nov 7.
PMID: 31699882

Evolving neoantigen profiles in colorectal cancers with DNA repair defects.

Rospo G, Lorenzato A, Amirouchene-Angelozzi N, Magrì A, Cancelliere C, Corti G, Negrino C, Amodio V, Montone M, Bartolini A, Barault L, Novara L, Isella C, Medico E, Bertotti A, Trusolino L, Germano G, Di Nicolantonio F, Bardelli A.

Genome Med. 2019 Jun 28;11(1):42. doi: 10.1186/s13073-019-0654-6.
PMID: 31253177

Abstracts

Abstract B069: Temozolomide drives mismatch repair deficiency and fosters neoantigen generation in tumor cells

Vito Amodio, Giovanni Grmano, Ludovic Barault, Simona Lamba, Giuseppe Rospo, Alessandro Magrì, Federica Maione, Giovanni Crisafulli, Carlotta Cancelliere, Giulia Lerda, Alice Bartolini, Giulia Siravegna, Benedetta Mussolin, Roberta Frappolli, Monica Montone, Giovanni Randon, Filippo de Braud, Nabil Amirouchene Angelozzi, Silvia Marsoni, Maurizio D'Incalci, Armando Orlandi, Enrico Giraudo, Andrea Satore-Bianchi, Salvatore Siena, Filippo Pietrantonio, Federica Di Nicolantonio and Alberto Bardelli

DOI: 10.1158/2326-6074.CRICIMTEATIAACR18-B069 Published February 2019

Abstract A120: Adaptive mutability of colorectal cancers in response to targeted therapies

Mariangela Russo, Giovanni Crisafulli, Alberto Sogari, Nicole Megan Reilly, Sabrina Arena, Simona Lamba, Alice Bartolini, Vito Amodio, Alessandro Magrì, Luca Novara, Ivana Sarotto, Zachary Nagel, Cortt Piett, Alessio Amatu, Andrea Sartore-Bianchi, Salvatore Siena, Andrea Bertotti, Livio Trusolino, Federica Di Nicolantonio and Alberto Bardelli

DOI: 10.1158/1535-7163.TARG-19-A120 Published December 2019